THE UNIVERSITY OF WESTERN ONTARIO
DEPARTMENT OF CIVIL AND
ENVIRONMENTAL ENGINEERING

Water Resources Research Report

Climate Change Impact on Flood Hazard in the Grand River Basin, Ontario, Canada

By:

Abhishek Gaur
and
Slobodan P. Simonovic

Report No: 084
Date: December 2013

ISSN: (print) 1913-3200; (online) 1913-3219;
ISBN: (print) 978-0-7714-3063-3; (online) 978-0-7714-3064-0;

CLIMATE CHANGE IMPACT ON FLOOD HAZARD IN THE GRAND RIVER BASIN, ONTARIO, CANADA

By

Abhishek Gaur

and

Slobodan P. Simonovic

Department of Civil and Environmental Engineering

Western University, Canada

Dec 2013

EXECUTIVE SUMMARY

Rapidly changing climatic conditions across the globe are having an impact on key climate variables and the hydrologic cycle. Changes in magnitude and frequency of peak flow patterns have been noted in the rivers worldwide from past few decades. The associated risk is projected to increase many folds during the 21st century. Therefore, it is necessary to quantify these impacts for effective water resource planning and management in future. Methodology chosen to do so should be able to capture variations in climate variables at fine temporal, spatial and distributional scales. Also, it should be able to cover uncertainties associated with future climatic, socio-economic and physiographic projections. In this study, a discussion of the same has been started with a focus to estimate changes in occurrence probability of flow extremes in future. Based on the discussion, a methodology has been developed to estimate changes in flood hazard. It is proposed that all future projections made by climate models should be considered in the analysis. Model data should be pre-processed to improve its spatial, temporal and distributional resolution keeping in mind that the changes projected by them shouldn't be significantly altered. Pre-processed climatic data can be used to generate flows. Independent extreme flow events are identified and their reoccurrence probabilities are compared with that of historical flow data extremes to get an estimate of the range of projections plausible in future.

Investigation of practical utility of the developed methodology has been tested using the Grand River basin, Ontario, Canada as a case study. A huge array of projections is obtained for future. It is suggested that the band of interest should be extracted wisely out of them depending on the usage of results.

Dedicated to my *Teachers*, *Parents* and *Bhagwan*

TABLE OF CONTENTS

LIST OF FIGURES

LIST OF TABLES

List of Acronyms

AET	Actual Evapo-Transpiration
AM	Annual Maximum
AR4	Fourth Assessment Report (Issued by the IPCC)
CDCD	Canadian Daily Climate Data
CDF	Cumulative Distribution Function
CF	Change Factor
CMIP	Coupled Model Inter-comparison Project
DOS	Disk Operating System
ECDF	Empirical Cumulative Distribution Function
FORTRAN	(IBM Mathematical) FORmula TRANslating System
GCM	Global Climate Model
GHG	Green House Gas
GHM	Global Hydrologic Model
GPD	Generalised Pareto Distribution
GRCA	Grand River Conservation Authority
IEP	Interception EvaPoration
IPCC	Intergovernmental Panel for Climate Change
MME	Multiple Model Ensembles
NARR	North-American Regional Reanalysis
NCAR	National Centre for Atmospheric Research
NCDIA	National Climate Data and Information Archive
NCEP	National Centres for Environmental Protection
NetCDF	Network Common Data Forum
PDSI	Palmer Drought Severity Index
PDF	Probability Distribution Function
PET	Potential Evapo-Transpiration
POT	Peak Over Threshold
PWM	Probability Weighted Moments
Q-T	flood magnitude (Q) – return period (T)
R	Range
RAOBS	RAdiOsonde database
RCM	Regional Climate Model
RMSE	Root Mean Square Error
SRES	Special Report on Emission Scenarios
TAR	Third Assessment Report (Issued by the IPCC)
WG	Weather Generator
WCRP	World Climate Research Programme

1. INTRODUCTION

This chapter presents literature review followed by layout of the report. In the literature review section, climate change and its impact on key climate variables, for example temperature and precipitation, and on flow patterns are discussed on a global scale. Further, observed and projected impacts of climate change are discussed for the region of Canada with a focus on South-Western Ontario.

1.1 Literature review

According to IPCC, (2012) any detectable change in the state of climate which persists over a considerable period of time (more than a decade) can be referred to as climate change. Both natural (such as periodic changes in solar irradiance) and man-made (such as GHG emissions, changes in land-use patterns etc.) sources can be responsible for it. However, role of anthropogenic factors towards climate change has been found to be significant as compared to other sources (Huber & Knutti, 2011; IPCC,2007).

Carbon-di-oxide (CO_2) is an important greenhouse gas, whose concentration in the atmosphere has increased significantly since the industrial revolution, primarily due to increased consumption of fossil fuels and rapid land use change. According to IPCC, (2007) atmospheric concentration of CO_2 in 2005 was higher than that experienced in the past 6,50,000 years and annual CO_2 growth rate continues to increase each passing year. Similar trends have also been recorded for other greenhouse gases such as methane and nitrous oxide. Due to the changes in environmental chemistry, changes in the mean, standard deviation and extremes of key climate variables are being observed. There has been an unprecedented increase in global mean temperatures in the last 25 years. Changes in precipitation patterns have also been noted

worldwide. A change in climate variables other than precipitation and temperature have also been reported (IPCC, 2007).

Since hydrologic behaviour of a catchment is governed by feedbacks from various climatic and ecologic variables, relationships between them are difficult to formulate. An extensive Canada-wide study highlighting this relationship has been performed by Whitfield & Cannon, (2000). They grouped changes observed in precipitation, temperature and streamflow between the decades 1976-1985 and 1986-1995 into different classes or clusters. After analysing the spatial distribution of these climatic and hydrologic clusters obtained from 210 temperature, 271 precipitation and 642 hydrology stations, they noted distinct linkages between climate variables, hydrologic responses of streams and ecozones within Canada. The study also highlights that even small changes in climate variables may result in significant changes in a region's hydrologic characteristics.

By reconstructing monthly discharges of the largest worldwide rivers, Labat, Godd, Probst, & Guyot, (2004) estimated a 4% increase in global runoff every 1ºC rise in global temperatures over the last century. Further, IPCC, (2007) projects a range of 1.8ºC (low emission scenario) to 4ºC (high emission scenario) in global mean temperature change (relative to temperatures observed during 1980-1999) for the 21st century. It is anticipated that this change in global mean temperature will produce unprecedented changes in hydrologic regimes across the globe.

The impact of climate change has been identified on precipitation and temperature extremes. According to IPCC (2012) there is a strong likelihood that since 1950, the number of cold days and nights has decreased, whereas the number of hot days and nights has increased globally. An increase in anthropogenic emissions has been identified as the most likely cause for

this change. Further, it is projected that following SRES A2 and A1B scenarios, by the end of 21st century, a 1 in 20 year return period annual hottest day event may become 1 in 2 year return period event (except for high latitudes of Northern America where it will become a 1 in 5 year event). Changes in precipitation extremes have also been detected worldwide. Most consistent increases in precipitation extremes have been noted across the North American sub-continent. It has been projected that towards the end of 21st century, a 1 in 20 year return period annual maximum 24-hour precipitation rate event will change to 1 in 5 to 1 in 15 year return period event.

Change in frequency of flood and drought events has also been reported. Since 1950, droughts have become more frequent and intense in southern Europe and western Africa, while they have become less frequent and intense in central North America and northwestern Australia (IPCC, 2012). In the case of flooding, precise identification of changes in historical flooding trends and their attribution to climate change has not been possible as of yet. However, there is evidence suggesting a shift in the timing of spring peak flows. Due to excessive warming and subsequent melting of winter snow accumulations, spring peak flows of the past have been detected to occur during winters or early springs. Further, global (Hirabayashi et al., 2013; Hirabayashi et.al. 2009) and continental scale (Dankers & Feyen, 2009) studies project an increase in flood hazard..

Changing climate has induced changes in temperature and precipitation patterns across Canada. These changes vary spatially, with frequency, duration and intensity of cold spells decreasing around western and increasing around eastern regions of Canada (Groisman et al., 2002; Shabbar & Bonsal, 2003). Winter warm spells are increasing in both frequency and duration across all of Canada, with one exception in the extreme north-eastern regions where warm spells are becoming shorter and less frequent (Shabbar & Bonsal, 2003). Precipitation has increased in almost all parts of Canada during the last 50 years. An average increase of 5% has been observed

in annual total precipitation for the entire country, while an increment of 12% has been observed in southern Canada indicating that the changes in precipitation are not uniform spatially. Further, precipitation has been found to increase during spring, summer and autumn while the ratio of snowfall to total rainfall has been decreasing in winter and spring especially along the western part of the country (Barrow, Maxwell, & Gachon, 2004). This observation is consistent with the warming trends observed along the western regions of Canada.

Changes in major climatic variables such as temperature and precipitation also affect the flow patterns of Canadian rivers. Annual maximum and mean daily flows are significantly increasing in northern British Columbia, Yukon Territory and southern Ontario. On the other hand, a decreasing trend is observed in the southern regions of British Columbia (Environment Canada, 2004). Studies also estimate a decrease of approximately 10% in annual river discharge in the period 1967 to 2003 for rivers situated in the northern regions of Canada (Déry, 2005). More recently, an extensive study analysing present and projected future flows of ten rivers with varying geography, ecosystem and drainage basins situated across Canada (Figure 4). They projected a steady and decreasing flow trends across all the selected rivers except River Nipigon (WWF-Canada, 2009).

The number of flooding events has increased over the last 50 years, with 70% of flooding events occurring after 1959. It has also been estimated that 62% of these flood disasters have been caused by snowmelt runoff, storm rainfall or their combinations (Brooks *et al*., 2001). A detailed study of the 168 flood disasters between 1990 and 1997 revealed that most of these occurred in densely populated areas. For example, it is found that 62% of these disasters occurred in four intensely populated provinces: Ontario (37 events), New Brunswick (26 events), Québec (23 events) and Manitoba (18 events) while relatively few disasters are observed in sparsely populated

provinces of Northwest Territories (5 events), and Yukon (3 events) (Shrubsole, Lacroix, & Simonovic, 2003). This suggests that the amount of *flood risk* (defined as the product of flood probability or hazard, and exposure of capital and population to that hazard) is gradually increasing across Canada.

Historical records suggest a shift towards milder winter and warmer summers in the south-western regions of Ontario. This region experiences frequent precipitation extremes due to large amounts of water vapour in the atmosphere because of close proximity of the Great Lakes. Between 1979 to 2004, south-western Ontario experienced the greatest number of heavy rainfall events within the province of Ontario (Report of the Expert Panel on Climate Change Adaptation, 2009). Temperature and precipitation means and extremes are projected to further increase in future across south-western Ontario. A decreased annual runoff, increased winter and spring flows, lower summer and fall flows, and increased frequency of high flows is projected for the 21st century in this region (Lemmen et. al., 2008). Due to high population density and high industrialisation in the region, south-western Ontario is considered to be at highest degree flood risk in the entire province. This has prompted several climate change studies in the region (Cunderlik and Simonovic, 2005; Cunderlik and Simonovic, 2007; Prodanovic and Simonovic, 2007; Solaiman et.al. 2010; Eum and Simonovic, 2012; King et.al., 2012; Solaiman et.al., 2012; Das and Simonovic, 2012) and highlights the importance of an extensive climate change impact study for this region.

1.2 Layout of the report

In this report, chapter 2 describes the methodology adopted while performing climate change impact analysis on Grand River at Brantford catchment. Application of the selected methodology

on Grand River basin is provided in chapter 3, results and discussions are provided in Chapter 4. Conclusions are summarised in Chapter 5, which is followed by references and appendices.

2. METHODOLOGY

Global Climate Models which have daily precipitation, t_{mean}, t_{max} and t_{min} datasets available for historical (1961-2000) and future timelines (2050s and 2090s) from the Coupled Model Intercomparison Project-Phase 3 (CMIP3) ensemble are selected for analysis. Scenarios A2, B1 and A1B are used to cover the uncertainty projected by future greenhouse gas emission scenarios.

Historical and future GCM data, corresponding to selected GCM-scenario combinations is bias-corrected using statistical bias correction approach. Statistical downscaling is performed on bias-corrected GCM data by following a change factor approach and using a weather generator. A set of 20 plausible future precipitation and mean temperature timeseries are generated corresponding to each GCM scenario combination for future timelines 2050s and 2090s using a non-parametric weather generator M3EB (Srivastav and Simonovic, 2013). Simulated future precipitation and temperature combinations most likely to produce hydrological extremes are selected for streamflow generation.

Hourly precipitation and temperature timeseries corresponding to selected combinations are used as inputs into a semi-distributed hydrologic model and future flow series are generated by performing continuous hydrological simulation. Statistical analysis is performed on historical observed and future simulated flowseries. Flow peaks are selected using Peak Over Threshold (POT) method and a Generalised Pareto Distribution (GPD) is used to fit the selected flood peaks. Flood frequency analysis is performed and results for 2, 5, 10, 25 and 100-year return period floods

are compared for historical and future time-periods to estimate the impact of climate change on flow peaks across the catchment.

2.1 Key features of selected methodology

Modelling climate change impact on water resources is a complex task. Steps involved in a typical climate change impact analysis process are outlined in Figure 1. Uncertainties exist at each step of the process. Six major sources of uncertainty involved have been identified in the literature. Uncertainties may arise from Global Climate Model structure, future greenhouse gas emission scenarios, downscaling of GCM outputs, hydrological model structure, hydrological model parameters and the internal variability of the climate system (Kay, Davies, Bell, & Jones, 2009). However, uncertainties may also exist outside the paradigm of these six primary sources. Chen, Haerter, Hagemann, & Piani, (2011) considered the decade used for deriving bias correction parameters as one of the three major sources of uncertainties associated. Hagemann et al., (2011) notes that uncertainty associated with bias correction step may be of an order equal to that associated with climate model projections. Climate model initial conditions, land-use change, natural variability of climate, choice of appropriate change factor methodology, choice of flood frequency analysis methodology are only some of many other uncertainties associated with the climate change impact analysis process.

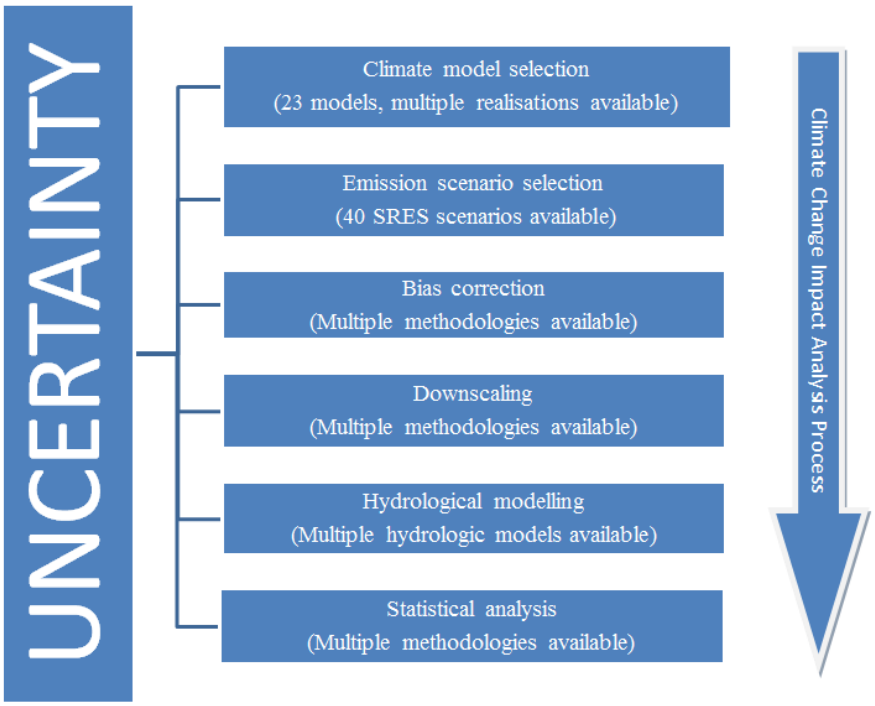

Figure 1 Steps and uncertainties involved in the climate change impact analysis process

Since it seems impossible to capture all the uncertainties associated with the process, identification and accounting for primary sources of uncertainty becomes important. Several studies have been performed to quantify relative contributions of different sources of uncertainty towards the total uncertainty. To this end, Jung, Chang, & Moradkhani, (2011) compared five sources of uncertainty viz. those related to GCM structures, future GHG emission scenarios, land-use change scenarios, natural variability and hydrologic model parameters to estimate their relative impact on flood frequencies across two catchments with different extents of urbanisation. Kay et al., (2009) analysed uncertainties contributed by GCM structure, downscaling methodologies, hydrological model structure, hydrological model parameters and internal variability of climate system and compared their impacts on flood frequency across two catchments in England.

Kingston & Taylor, (2010) compared uncertainties associated with GCM structures, climate variability and hydrologic parameterisation to quantify the impact of climate change on freshwater resources in the upper Nile basin in Uganda. Wilby & Harris, (2006) simulated future low flow scenarios for Thames River (UK) by using four GCMs, two GHG scenarios, two statistical downscaling techniques, two hydrological model structures and two sets of hydrological model parameters. In almost all such studies, uncertainty associated with future climate projections has been identified as the most significant component of total uncertainty. Therefore, the *major focus of this study is towards encompassing future climate projection uncertainty* i.e. uncertainties contributed by GCM structure and future greenhouse gas scenarios, while other sources of uncertainty are left to be addressed in future work.

Changes in climate extremes have been projected to be many folds higher than climate normals in future (IPCC, 2012). An increase in the intensity and frequency of climate extremes is projected to have significant socio-economic and environmental impacts on society in future. For the same reason, IPCC, (2012) emphasises the need for accurate prediction of future climate extremes. Therefore, another region of focus of this study is *to be able to capture changes associated with entire distributions of climate variables*. Different bias correction methodologies correcting entire distributions of climate model data have been proposed and are found to perform better than traditional methods correcting data means (Piani et al., 2010). Further, multiple change factors associated with specific percentiles of whole distribution have been found to be more effective in transferring changes projected by climate models than a single mean change factor (Anandhi et al., 2011). These methods and others available from literature are employed in this study for the synthesis of future climate variable distributions in the best possible manner.

An appropriate temporal scale has been selected for this study. Although majority of climate change studies have been performed on monthly or yearly timescales, the importance of evaluation of climate models on a daily temporal scale is highlighted in Perkins et al., (2007). Similar recommendations supporting the use of daily change factors over monthly change factors is made in King, (2012). Therefore, a *daily temporal scale is adopted for use in the present study*.

2.2 Climate change impact analysis process

A detailed explanation of three major steps followed while performing this study: (i) generation of future climate projections, (ii) pre-processing of GCM data and (iii) generation and analysis of future streamflow projections.

2.2.1 Generation of future climate projections

In this section, steps performed to generate future climate data at the area of interest have been described. These include selection of Global Climate Models (GCMs) and future emission scenarios for analysis, spatial interpolation of climate model data at the gauging stations of interest and filling-in of the historical observed data using spatially interpolated reanalysis data.

Selection of Global Climate Models (GCMs) and emission scenarios

Atmosphere Ocean Global Climate Models (AOGCMs) are the approximate mathematical representations of physical processes occurring within the climate system. They provide us with the best possible estimates of historical and future climate data worldwide. A group of climate models have been identified and outlined in IPCC, 2007 and their number, complexity and effectiveness in simulating climate is increasing gradually. Till date, none of them has been found to be able to predict earth's climate accurately. Three major reasons have been identified to be

responsible for it: a) limited theoretical knowledge about the processes occurring within the climate system, b) structural model uncertainty i.e. missing or approximated processes included in the models and c) parameter model uncertainty i.e. inability to depict complex natural processes perfectly using a set of parameter values (Knutti et al , 2010).

A total of forty scenarios were proposed in the Third Assessment Report (TAR) to encompass future emission uncertainty. Out of them, the SRES scenarios A2, A1B and B1 have been employed in the CMIP3 to prepare "WCRP CMIP3 multi-model datasets" for future (Meehl et al., 2007). They represent "high", "medium" and "low" scenarios with regards to full range of emission forcings projected by the SRES scenarios. More recently, CMIP5 data results are based on Representative Concentration Pathways (RCPs), in which four representative paths RCP8.5, RCP6.0, RCP4.5 and RCP2.6, leading to a 2100 radiative forcing level of 8.5 W/m^2, 6 W/m^2, 4.5 W/m^2 and 2.6 W/m^2 respectively have been introduced. In both the SRES as well as RCP scenarios, attempt has been made to capture the variability in future emissions as effectively as possible. Future climate data is generated following one of these plausible future emission scenarios.

To account for the uncertainty associated with climate model outputs, an ensemble of their results or Multiple Model Ensembles approach, MMEs has been recommended for usage over a single or selected set of model output (IPCC, 2007). The selection of climate models is generally restricted by the unavailability of climate data for the climate variable of interest within the time-period of interest. Climate variables that are generally considered while performing future flow projection analysis are precipitation (*ppt*), mean temperature (t_{mean}), maximum temperature (t_{max}) and minimum temperature (t_{min}). Availability of climate data varies across these climate variables and models with consistent climate data across all four climate variables, in both future timelines, can only be selected for analysis.

Table 1 Summary of CMIP3 precipitation, mean temperature (t_{mean}), maximum temperature (t_{max}), minimum temperature (t_{min}) datasets for historical and future (2045-2065 and 2081-2100) timelines

Climate Variables	**Historical**	**Future**		
		A1B	*A2*	*B1*
ppt	22, 1910	21, 1550	21, 1240	21, 1480
t_{mean}	22, 1920	21, 1560	21, 1240	21, 1440
t_{max}	21, 1640	19, 1240	19, 960	19, 1200
t_{min}	21, 1640	19, 1240	19, 960	19, 1220

After analysing the data available from the CMIP3 project mentioned in Table 1, it is found that only sixteen models (listed in Appendix A) have complete set of daily *ppt*, t_{mean}, t_{max} and t_{min} data available, for one or more future scenarios, corresponding to one or more runs in both historical and future timelines. This highlights the need for consistent data across climate variables for the entire period necessary to be considered in the analysis. Need for data consistency across climate models has been identified and has been considered while preparing the new climate model intercomparison project CMIP5 results (Taylor et al , 2007).

As discussed before, a large number of climate models as well as emission scenarios have been outlined to capture uncertainty associated with future climate. New (or updated) models and scenarios are being proposed continuously, which are adding further towards already vast uncertainty in climate projections. Since each realisation result of every proposed model and scenario combination is equally plausible in the future, none of them can be ignored from the analysis. Accounting for all such projections is a herculean task and demands enormous amount of time and computation resources for performing even a single climate change study in the area of interest.

To reduce the workload, model-scenario combinations encompassing the entire range of changes projected by climate models can be selected for analysis. A workshop conducted by Environment Canada (EC) in Quebec (Mortsch, 2011) recommended two methods for the same. They are referred to as *scatter plot method* and *percentile method*. Similar recommendations and conclusions are drawn by the Ministry of Natural Resources, Ontario at the Conservation Ontario Climate Change Workshop (Garraway, 2011).

Both methods mentioned above have been used to encompass climate projection uncertainty in numerous studies across Canada. While analysing future temperature and precipitation trends in Alberta (Barrow & Yu, 2005), five model-scenario combinations, i.e. coldest and wettest (NCARPCM-A1B), coolest and driest (CGCM2-B2), warmest and wettest (HadCM3-A2), warmest and driest (CCSR-A1FI) and the median conditions (HadCM3-B2) were chosen to capture uncertainty associated with future projections. In a similar study performed in the province of Saskatchewan (Lapp et al, 2008), model-scenario combinations projecting warmest-wettest, warmest-driest, coolest-wettest, and coolest-driest future climates around the South Saskatchewan river were selected for analysis.

Scatter-plot method

In the scatter-plot method, GCM-scenario combinations most likely to produce hydro-climatic weather extremes in future are selected for the analysis. Percent mean changes in precipitation and absolute temperature as projected in future by each GCM-scenario combination are plotted and scenarios corresponding to extreme future precipitation-temperature scenarios are selected (Mortsch, 2011). Figure 2 illustrates the selection of model-scenario combinations for 2050s from all scenarios associated with sixteen climate models selected for analysis. Selected

extreme scenarios (in green/red) correspond to wet-hot, wet-cold, dry-hot and dry-cold precipitation-temperature combinations.

Percentile method

In percentile method, selection is made to capture the whole range of changes projected by GCMs. Percent changes in precipitation are plotted against absolute changes in temperature. Future GCM-scenario combinations corresponding to 5^{th}, 25^{th}, 50^{th}, 75^{th} and 95^{th} percentiles of changes in both climate variables are selected (Mortsch, 2011). Figure 3 illustrates the selection of model-scenario combinations for 2050s from all scenarios associated with sixteen climate models selected for analysis.

An important area of discussion associated with the application of these plotting methodologies is to ascertain an appropriate spatial, temporal and distributional scale at which the changes (projected by GCMs) should be calculated. In Figure 2, GCM-scenario combination selection is made using scatter plot method for data projected by the sixteen GCMs selected before. Scenarios in red have been selected using changes projected in mean and scenarios in green have been selected using changes projected in mean of data lying above 99^{th} percentile value. Any common selection is plotted in both the colours. Similarly, in Figure 3, selection is made using percentile method using mean and mean above the 99^{th} percentile changes. A clear difference between the selected scenarios is visible in both the cases. It indicates that the selection does depend on the distributional scale selected for analysis. Therefore, it is important to select for a suitable distributional scale based on which the selections should be made. We recommend that the scale should be selected depending on the kind of analysis being performed. For example, in a

study focussing on the quantification of climate change impact on flood frequency scenarios in green will be preferable to those in red.

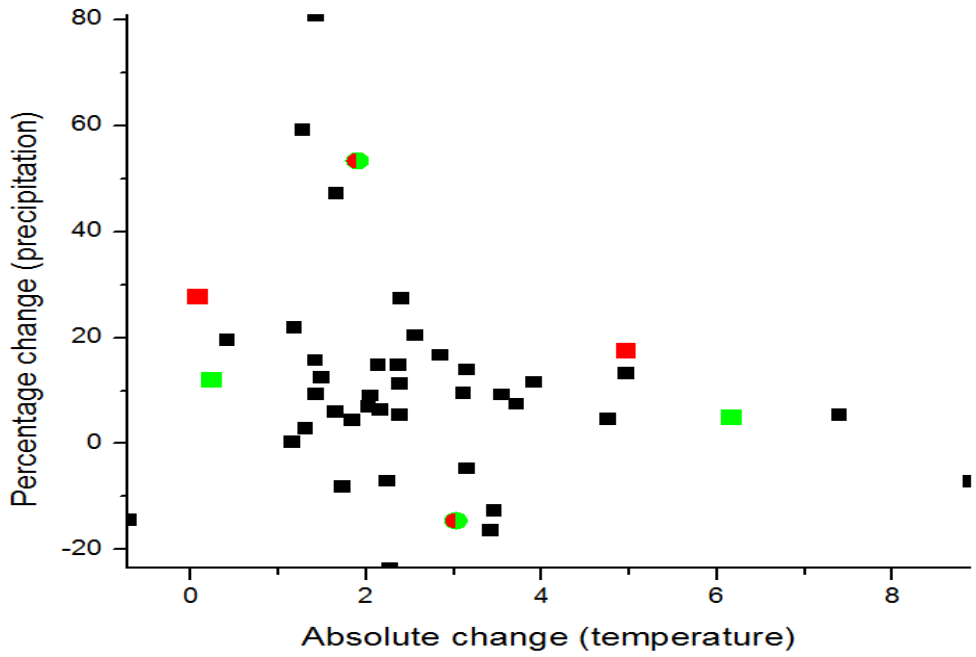

Figure 2 GCM-scenario combination selection using scatter-plot method. Scenarios highlighted in red are selected based on mean change while those in green are selected based on mean above 99th percentile change

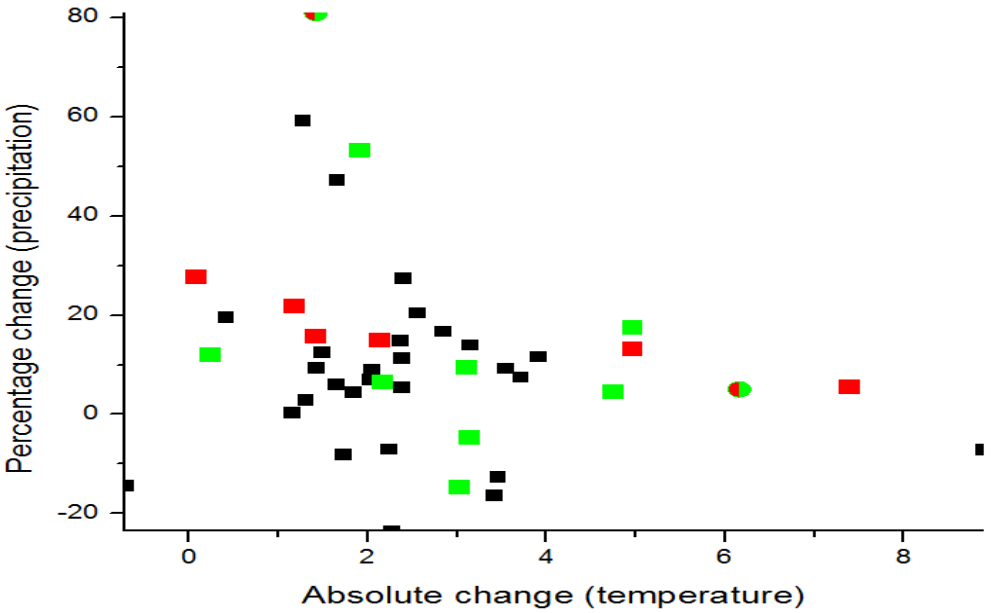

Figure 3 GCM-scenario combination selection using percentile method. Scenarios highlighted in red are selected based on mean change while those in green are selected based on mean above 99th percentile change

Further, spatial extents of a single GCM grid are very large as compared to that of a typical catchment. Small or medium size catchments, like the one used in our study are generally engulfed within one grid cell of the GCM data. To associate changes within one or few grid cells completely or partially encompassing the area of interest, can give misleading information about the changes projected there because GCM data within one grid cell has been found to be influenced by the surrounding grid cells as well (Masson & Knutti, 2011). Plots shown in Figures 2 and 3 have been created by dividing the Province of Ontario into three sections based on historical climate trends across the province (process involved in formation of the three sections is explained in Appendix A). Distinctly different sets of scenario have been obtained for all three sections. This reiterates the need for choosing an appropriate spatial scale before making GCM-scenario combination selections.

Selected scenarios also vary with the time-period considered for analysis. For the plots shown in Figure 2 and 3, data corresponding to period 1961-2000 has been used as the baseline data and 2045-2065 has been used as future data. Different plots, and hence selections are obtained if different period for baseline or future data are considered.

In summary, it is important to take into consideration climate projections made by each GCM while performing climate change impact studies. Although the choice of GCMs is limited by shortage of consistent data across climate variables, there are still a huge number of GCM-scenario combinations to be considered for analysis. The entire range of changes projected by them can be encompassed by selecting a few combinations out of them using plotting methodologies like scatter-plot and percentile method. Selected scenarios, however, depend on the spatial, temporal and distributional scale selected for analysis.

Preparation of continuous, point location climate data

Gridded climate model data can be spatially interpolated at a location of interest using interpolation methods like inverse distance square method. According to this method, data at a particular location is inversely proportional to the square of its distance from the nearest model grid point. The distance of point of interpolation is found out from four nearest reanalysis data grid points surrounding it. A simple formula, shown in Equation 2.1 is then used to calculate weight associated with each grid point. Interpolated value at a particular location (v_i) is calculated by finding the sum of weighted means of climate data at all four grid points (v_j) using Equation 2.2.

$$w_j = \frac{{}^{1}/_{d_j^2}}{{}^{1}/_{d_1^2} + {}^{1}/_{d_2^2} + {}^{1}/_{d_3^2} + {}^{1}/_{d_4^2}} \qquad (2.1)$$

$$v_i(t) = \sum_{j=1}^{4} w_j * v_j(t) \quad (2.2)$$

where d_1, d_2, d_3 and d_4 are the distances of the location of interpolation from four nearest grid points and w_j is the weight calculated for j^{th} grid point.

Historically observed precipitation and temperature datasets are often found incomplete or intermittent over the baseline period. These can be filled-in using spatially interpolated National Centres for Environmental Protection (NCEP)/National Centre for Atmospheric Research (NCAR) or North-American Regional Reanalysis (NARR) data. Interpolation of reanalysis data at a particular climate gauging station location can be done using the inverse distance square method as explained before.

2.2.2 Pre-processing of GCM data

Climate model datasets are associated with low spatial, temporal and distributional resolution. They have typical horizontal spatial resolutions of 2° x 2° which is close to 220 km x 220 km. This means that physiographic characteristics of such a huge area are approximated into one grid cell of the climate model data. Spatial extents of grid points exceed the catchment scales at which climate change studies are typically performed. Similarly, datasets are available in yearly, monthly and more recently in daily time steps. However, most hydrologic models typically require hourly datasets for generating streamflows. Further, climate data obtained from GCMs are associated with some time-independent component of model errors called biases (Ehret et al, 2012). These biases are evident when simulated climate model data for baseline are compared with historical observed data at the same location. To make the raw climate data usable for catchment scale hydrological analysis, methods such as bias-correction, downscaling and temporal disaggregation are employed.

Bias correction of gridded GCM climate data

While performing climate change impact studies, bias associated with climate model data can be roughly but safely, defined as the time independent component of model error or the component of model error which remains constant throughout the length of datasets (Ehret et al. 2012, Chen et al. 2011). The need for bias-correction step while performing climate change impact studies has been advocated by many researchers (for example, Muerth et al. 2012) and on the other hand, has been criticised by some (for example, Vannitsem 2011). A major argument against the application of bias-correction is that most methods employed to do so are purely statistical in nature and lack a sound physical basis i.e. they are not governed by the laws of physics (Haerter et al, 2011). Therefore, it is argued if they should be used to bias-correct GCM outputs, which are prepared taking into consideration complex hydro-meteorological, atmospheric and land-surface interactions prevalent within Earth's climate system.

Importance of this particular step and the methodology chosen to do so, can be realised by analysing the impact of bias-correction on projected future streamflow patterns. Sharma et al. (2007) applied bias-correction to spatially interpolated daily precipitation data in the Ping river basin (Thailand) and analysed its impact on the simulated discharge output. They found that the root mean square error (RMSE) between observed and simulated discharge series changed from 172 m^3/s to 93 m^3/s. In another study, after bias-correction of gridded datasets from three GCMs for two scenarios and noting the changes in hydrological output from two Global Hydrologic Models (GHMs), Hagemann et al. (2011) concluded that bias correction step improves the simulated runoff patterns in most catchments considered in the analysis. It has also been pointed out that the uncertainty associated with bias-correction step can be of an order similar to that of

GCM projections. These findings highlight the need for, and caution required, while selecting and applying a bias-correction methodology.

The purpose of bias correction step is to modify the climate model data in a way the correlation of model baseline data with observed data improves. Methods employed to do so range from those correcting just the means (Fowler and Kilsby, 2007; Schmidli et al, 2006) to those correcting entire distributions of climate data (Ines & Hansen, 2006; Piani et al., 2010). Most recent efforts are towards including changes in bias correction parameter statistics between present and future (Watanabe et al., 2012), effects of multiple timescales (Haerter et al., 2011), correlation between multiple variables being corrected (Piani & Haerter, 2012).

Correction of probability distribution functions (PDFs) of climate variables has been advocated in recent research (Haerter et al., 2011; Piani et al., 2010; Piani et al., 2009). Methods used to do so are generally referred to as "quantile mapping", "histogram equalisation" or "rank matching" methods for correcting the GCM bias (Maraun et.al. 2010). Several studies comparing effectiveness of multiple bias correction methodologies towards bias correction of climate model data have been performed. By comparing seven downscaling and bias correction methodologies, Jakob Themeßl et al., 2011 recommends the usage of quantile mapping methodology for bias correction, especially while analysing climate extremes. Teutschbein & Seibert, 2012 test six bias correction methodologies of varying complexity in a non-stationary climate setting and concluded that distribution based methodologies perform best under a changing climate.

One such methodology is statistical bias correction method explained in Piani et al., (2010). In this method, climate model data (X_{mod}) is transformed so that the intensity histogram of corrected model baseline data (X_{cor}) matches with the intensity histogram of observed data (X_{obs}) using

transfer functions. Transfer functions for a particular climate variable are estimated by first calculating the cumulative distribution function (CDF) of modelled and observed historical data and then, by finding correlation between them such that for each point in the distribution $CDF_{mod}(X_{mod}) = CDF_{obs}(X_{obs})$.

There are a few clear advantages of applying statistical bias correction methodology over traditional methods. The methodology can be used to correct a) mean only (when only additive transfer functions are used), b) mean and standard deviation only (when linear transfer functions are used) c) entire distributions (when exponential transfer functions are used) of model data. In other words, an appropriate level of complexity can be selected in transfer functions, to obtain the desired level of accuracy in results.

Estimation of monthly bias correction parameters for precipitation data

The transfer functions chosen for bias-correction should have minimal degrees of freedom so that they are robust and constantly valid over the period of analysis. Piani et al., (2010) suggested three transfer functions for bias-correcting daily precipitation data. Out of them, linear and exponential transfer functions (Equation 2.3 and 2.4) have been used in this study.

$$x_{cor} = a+bx \tag{2.3}$$

$$x_{cor} = (a+bx)\left(1 - e^{(-(x-x_0))/\tau}\right) \tag{2.4}$$

where, a is the additive correction factor, b is the multiplicative correction factor, τ is the rate of approach of attaining the asymptote, and x_0 is the dry day correction factor. It represents the maximum precipitation below which modelled precipitation is assumed to be zero. Also, x_0=-a/b.

It is suggested in Piani et al., (2010) that transfer functions are well approximated by linear functions (Equation 2.3) at higher precipitation intensities. However, to accommodate for a systematic change of slope at lower intensities, an exponential form of transfer function is also suggested (Equation 2.4). This function has an exponential tendency to the asymptote $(a+bx)$, where the rate of approach to the asymptote is τ and dry day correction factor is x_0. A combination of these two transfer functions is found to produce reasonable results in a global analysis performed in Piani et al., (2010). Similar results have been found by (Rojas et al., 2011) while correcting daily Regional Climate Model (RCM) precipitation and temperature time series over a pan-European scale. Therefore, a combination of linear and exponential transfer functions is used in this work to bias-correct daily precipitation following these steps:

1) Data falling under each month is extracted from the daily observed and model climate data.
2) Observed and modelled data is sorted in ascending order of intensities.
3) It is checked if at least 10% of the length of the observed record are contributed by wet days (>1mm of rainfall) and daily mean precipitation value is more than 0.01 mm/day. If any of these conditions are not met, a simple additive transfer function (equal to difference in means) is used to modify the modelled data.
4) If both the above conditions are met, for all wet days in observed record, linear transfer function (Equation 2.4) parameters are estimated by minimising the Root Mean Square Error (RMSE) of the fit obtained between model and observed climate data.
5) If fitted parameters $a<0$ and $1/5<b<5$, transfer function obtained from linear fit is used to modify climate model precipitation.
6) If above conditions on parameters are not fulfilled, minimisation of RMSE is performed to estimate four parameters a, b, τ and x_0 of exponential transfer function (Equation 2.4).

Estimating monthly bias correction parameters for temperature data

It has been explained in Piani et al., (2010) that bias-correction of maximum temperature (t_{max}), minimum temperature (t_{min}) and mean temperature (t_{mean}) data directly results in large relative errors in temperature skewness (t_{sk}) and temperature range (t_r). Therefore, it is proposed that bias correction of t_{max}, t_{min} and t_{mean} values should be performed indirectly by correcting t_{mean}, t_{sk} and t_r values first and then calculating t_{max} and t_{min} values using equations 2.9 and 2.10 respectively. Usage of linear transfer functions (Equation 2.3) is recommended while correcting t_{mean}, t_{sk} and t_r time-series (Piani et al., 2010) and are used in this study for bias correcting climate model temperature data.

Disaggregation of monthly bias correction parameters to daily timescale

Monthly bias correction parameters estimated before are disaggregated into daily timesteps using methodology explained in Piani et al., (2010). If interpolation is being done for adjacent months with similar transfer functions (for example, both fitted with either linear or exponential transfer functions), Equation 2.5 is used to calculate transfer function parameters for a particular day *d* within the two months. The equation calculates transfer function parameters for each day by finding weighted average of parameters obtained at the middle days of surrounding months. Weight assigned to transfer function of a particular month varies inversely with the time difference between the day in consideration and middle day of that particular month.

$$TF_d = \propto TF_{m-1} + (1-\propto)TF_m \qquad (2.5)$$

where, α is the weight assigned to month *m-1*. It depends on the distance of day *d* (in units of month) from middle day of month *m*, TF_d represents transfer function for day *d*, and TF_{m-1} and TF_m represent transfer functions at middle days of months adjacent to day *d*.

The process of disaggregation with dissimilar transfer functions in adjacent months (for example, with linear and exponential transfer functions) is a bit complex since it involves transition between different functional forms. An approximate solution for disaggregation of mixed transfer functions has been proposed in Piani et al., (2010) (Equation 2.6 to 2.8)

$$x_{cor,l} = a_l + b_l x \tag{2.6}$$

$$x_{cor,e} = (a_e + b_e(x - x_0))(1 - e^{(x-x_0)/\tau}) \tag{2.7}$$

$$x'_{cor} = (a' + b'(x - x'_0))(1 - e^{((x-x'_0)/\tau')}) \tag{2.8}$$

In the above equations,

$$a' = (1 - \alpha)a_e$$

$$b' = (1 - \alpha)b_e + \alpha b_l$$

$$x'_0 = (1 - \alpha)x_0 + \alpha(-\frac{a_l}{b_l})$$

$$ln\ \tau' = (1 - \alpha)\ell n\tau + \alpha \ln(0.5)$$

where, a_l, b_l denotes the additive and multiplicative correction factor for linear transfer function, a_e,b_e,x_0,τ denote the additive, multiplicative, dry day correction factor and correction factor for exponential transfer function,

a',b', x'_0, τ' denotes the additive, multiplicative, dry day correction factor and correction factor for interpolated transfer function, and α is the parameter which assumes values from 0 to 1. It is 0 when day in question falls in the middle of the month with exponential transfer function and is 1 when it falls in the middle of the month with linear transfer function.

Bias-correction of GCM climate data using daily transfer functions

The disaggregated daily transfer functions are used to bias-correct historical and future daily temperature and precipitation time series. Appropriate additive, linear or exponential transfer functions are applied on each day to correct model precipitation data. In the case of temperature, estimated daily linear transfer functions are used to bias-correct daily t_{mean}, t_{sk} and t_r timeseries. Timeseries of t_{max} and t_{min} is subsequently calculated using Equations 2.9 & 2.10,

$$t_{min}^{bc} = t_{mean}^{bc} - (t_{sk}^{bc} \times t_r^{bc}) \quad (2.9)$$

$$t_{max}^{bc} = t_{mean}^{bc} + t_r^{bc} \times (1 - t_{sk}^{bc}) \quad (2.10)$$

Statistical downscaling

Downscaling is a method for improving the spatial resolution of Global Climate Model (GCM) outputs. Two distinct groups of approaches can be followed for doing so. First group is known as the dynamic downscaling approach in which local physiographic information along with GCM boundary conditions are used to generate higher resolution Regional Climate Model (RCM) datasets. The dynamic downscaling process is highly computationally extensive. Further, dynamically downscaled results are governed significantly by associated GCMs (Raisanen et al., 2004) and so, they too are uncertain. Efforts are being placed currently to generate projections from multiple RCMs using boundary conditions from multiple GCMs to account for the associated uncertainty.

Another less computationally demanding approach for downscaling GCM data is known as statistical downscaling. It is based on the principal that regional data is dependent on large scale

climate state as well as local physiographic features (IPCC, 2001). Information regarding large scale climate state is generally extracted from the GCMs while several parametric, semi-parametric and non-parametric methods are employed to transfer this large scale information to regional scales. The process of statistical downscaling using weather generators can be sub-divided into two parts: *i)* calculation of future scaled climate variables and, *ii)* generation of future climate variable timeseries using a weather generator.

Historically observed climate variables are modified to include changes projected by climate models in future. These changes are incorporated into the observed data by using change factors (CFs) calculated from bias-corrected historical and future GCM data. CFs can be applied on different temporal scales (daily, monthly, seasonally or annually), can have different mathematical formulations (additive or multiplicative) and can vary in numbers (same or unique for different percentiles of a climate variable). Anandhi et al., 2011 gives a comprehensive overview of different change factor methodologies used in climate change impact studies. After performing a comparative analysis of different CFs, usage of multiple CFs over single CF, and of additive CFs over multiplicative CFs (unless the variable is bounded, in which case multiplicative CFs are to be used) has been recommended. This is because multiplicative change factors can give unrealistically high or low values in cases where the variable's value is very low. However, they found that usage of large number of bins (>=25) eliminates this difference (Anandhi et al., 2011). Keeping above factors in mind, following steps are followed in this study for generating future scaled climate variable data for precipitation and temperature:

1) Number of bins and distribution of variable percentiles across the bins is decided. Number of bins is kept >25. The distribution of variables can be uniform as well as non-uniform across selected bins.

2) Monthly empirical cumulative distribution functions (ECDFs) are calculated for bias-corrected historical and future GCM data.
3) For each month, means of the historical and future values falling within each bin is calculated.
4) Additive and multiplicative CFs are calculated for temperature and precipitation respectively for each month, at each bin, using equations 2.11 and 2.12.

$$CF_{add,b} = GCM_{f,b} - GCM_{h,b} \quad (2.11)$$

$$CF_{mult,b} = GCM_{f,b}/GCM_{h,b} \quad (2.12)$$

5) The historical observed data is distributed into an equal number of bins as the GCM data. CFs calculated for each bin are added or multiplied to the distributed observed values to obtain future scaled climate variable values.

Weather generators (WGs) are tools that generate synthetic series of climate data having characteristics similar to input data. They can be classified into three basic types i.e. parametric, semi-parametric and non-parametric WGs. Parametric weather generators typically employ Markov chains to simulate the occurrence of dry and wet days, and use probability distributions to calculate the amount of precipitation, temperature and other climate variables. The problem with this kind of weather generator is that they are heavily reliant on the statistical properties of the input data and generate climate series based on it. Since the statistical properties of historical and future climate data are expected to be different from each other, usage of parametric WGs for generating synthetic future climate series is clearly arguable. Semi-parametric WGs have both empirical as well as parametric components, which are used together in different ways to produce synthetic climate variable time series (King, 2012). Most of these WGs are single-site, single-

variable WGs, so the correlation between different climate stations as well as between different climate variables is lost in the generated future climate series.

Multisite multivariate weather generator model (M3EB) developed at Western University (Srivastav and Simonovic, 2013) is a non-parametric weather generator which can be used to generate synthetic multiple climate variable series at multiple locations. M3EB first converts the climate data into independent components orthogonally, uses Maximum Entropy Bootstrap procedure to generate synthetic replicates, and then transforms data back into original space by applying inverse orthogonal transformation. This weather generator has been found to preserve spatial and temporal precipitation, T_{max} and T_{min} data statistics at 27 stations across the Upper Thames River Basin (UTRB).

Multisite multivariate weather generator model (M3EB)

Following section presents the multisite multivariate weather generator model (M3EB) (Srivastav and Simonovic, 2013). Let the observed weather variables be represented by $\boldsymbol{W}$ and denoted by

$$W = \left[W_t^{1,1} W_t^{2,1} \ldots W_t^{n,1} \ldots W_t^{1,2} W_t^{2,2} \ldots W_t^{n,2} \ldots W_t^{1,k} W_t^{2,k} \ldots W_t^{n,k} \right] \tag{2.13}$$

where the superscript ‘n’ denotes the weather variable at site ‘k’ and ‘t’ is the index for time. In matrix form $\boldsymbol{W}$ can be expressed as

$$W = \begin{bmatrix} W_1^{1,1} & W_1^{2,1} & \ldots & W_1^{n,k} \\ W_2^{1,1} & W_2^{2,1} & \ldots & W_2^{n,k} \\ \vdots & \vdots & \ldots & \vdots \\ W_t^{1,1} & W_t^{2,1} & \ldots & W_t^{n,k} \end{bmatrix} \tag{2.14}$$

The total number of columns in matrix (2) is equal to N (n times k) and the total number of rows is equal to M (total number of days). The modeling steps include (i) preprocessing, (ii) generating replicates and (iii) post processing.

Preprocessing

1. Standardize the individual columns of matrix $\boldsymbol{W}$ following

$$w = \left[w^{1,1}\, w^{2,1} \ldots w^{n,1} \ldots w^{1,2}\, w^{2,2} \ldots w^{n,2} \ldots w^{1,k}\, w^{2,k} \ldots w^{n,k} \right] \tag{2.15}$$

where $w^{n,k}$ is $w^{n,k} = \dfrac{W_t^{n,k} - \overline{W^{n,k}}}{\sigma_{W^{n,k}}}$ (2.16)

in which, $\overline{W^{n,k}}$ and $\sigma_{W^{n,k}}$ represent the mean and the standard deviation respectively for each of the weather variables at the k[th] site (i.e., each column of matrix $\boldsymbol{W}$).

2. Apply orthogonal transformation, such that the matrix '$\boldsymbol{w}$' is fully uncorrelated. This is achieved by finding out the eigenvalues and eigenvectors of the covariance matrix obtained from the standardized dataset

$$r = Pw \tag{2.17}$$

where r is a scores matrix which is fully uncorrelated vector components also known as principal components (PC) and has a matrix size same as vector '$\mathbf{W}$', i.e. $(M \times N)$

$$r = \begin{bmatrix} r_1^{1,1} & r_1^{2,1} & \ldots & r_1^{n,k} \\ r_2^{1,1} & r_2^{2,1} & \ldots & r_2^{n,k} \\ \vdots & \vdots & \ldots & \vdots \\ r_t^{1,1} & r_t^{2,1} & \ldots & r_t^{n,k} \end{bmatrix} \tag{2.18}$$

P is the eigenvectors of the covariance matrix (Ω) and is given by

$$\Omega = COV(w) = \mathrm{E}\Delta\mathrm{E}^T \tag{2.19}$$

where E is the orthonormal eigenvector matrix or loadings and Δ is the diagonal eigenvalue matrix of size $(N \times N)$. The diagonal eigenvalue matrix (Δ) is arranged in

descending order, i.e., the first element of the matrix has the highest eigenvalue then the second and so on.

Generating Replicates –Bootstrap

3. The column of the first principal component is sorted in ascending order to create a rank matrix O_t.

4. From the rank matrix, compute intermediate points (P_t) using

$$P_t = \left(\frac{O_t + O_{t+1}}{2} \right) \quad for\ t = 1, \ldots, M-1 \tag{2.20}$$

5. For the lower and upper limit of the data use trimmed mean deviations (T_{mean}) from all consecutive observations as

$$T_{mean} = O_t - O_{t-1} \tag{2.21}$$

The lower limit is given as

$$P_0 = O_1 - T_{mean} \tag{2.22}$$

and the upper limit is determined as

$$P_M = O_M + T_{mean} \tag{2.23}$$

This ensures that the replicates generated are beyond the historical extremes.

6. The density is constructed, such that the ergodic theorem (mean preserving constraint) is satisfied. The following equations are used to calculate the desired mean

$$m_1 = 0.75O_1 + 0.25O_2$$

(2.24)

$$m_k = 0.25O_{k-1} + 0.5O_k + 0.25O_{k+1} \quad \forall\ k = 2,3,\ldots,t-1 \tag{2.25}$$

$$m_t = 0.25O_{t-1} + 0.75O_t \tag{2.26}$$

7. Uniform random numbers between 0 and 1 are generated and the sample quantiles of the density at those points are obtained and sorted accordingly.
8. Using the rank matrix in step 3, the sample quantiles are reordered. The step ensures that the temporal dependence of the historical structure is replicated.
9. Steps 4 to 8 are repeated, till the desired number of replicates of length 'M' are generated

Post-Processing

Assuming that the first component of the 'r' matrix (represented as $r_t^{1,1}$) is considered for generating the replicates in the transformed space (represented as $r_{t,rep}^{1,1}\ \forall rep = 1,\ldots,numrep$, where *numrep* is the total number of replicates generated), the post-processing continues through the implementation of the following steps .

10. Replace each replicate with the first component in scores matrix. For example to obtain first set of replicates in transformed space, replace $r_{t,1}^{1,1}$ in place of $r_t^{1,1}$ in matrix 'r' in Eq. 6 as shown below to obtain

$$r_1' = \begin{bmatrix} r_{1,1}^{1,1} & r_1^{2,1} & \dots & r_1^{n,k} \\ r_{2,1}^{1,1} & r_2^{2,1} & \dots & r_2^{n,k} \\ \vdots & \vdots & \dots & \vdots \\ r_{t,1}^{1,1} & r_t^{2,1} & \dots & r_t^{n,k} \end{bmatrix} \quad (2.27)$$

11. Using the modified scores matrix perform inverse orthogonal transformation to obtain synthetic weather variables at all sites.
12. Repeat steps 10 and 11, till the number of generated sequences are equal to total number of replicates to be generated.

Disaggregation of daily climate model data into hourly

As discussed before, climate model daily datasets need to be disaggregated to hourly timescale before they can be used for performing hydrological simulations. Capturing the hourly variability of climate variables accurately is important for simulating daily hydrological response of the catchment. Studies comparing different disaggregation methods, available in the literature, have been performed. For example, Debele et al., 2007 tested the efficacies of multiple methodologies for disaggregating daily wind speed, relative humidity, temperature and precipitation data into hourly timesteps. They found that cosine formula is suitable for disaggregating daily temperature data into hourly data. Merit of this method is that it is simple, easy to use and is virtually devoid of any parameters to calibrate. This implies that the method can be used freely in the baseline as well as future climatic conditions and hence, doesn't contradict with the principal of non-stationarity associated with climate change.

To obtain hourly temperature series, daily T_{max} and T_{min} series are used as inputs in the cosine function formula. A generalized expression of cosine formulae is expressed as,

$$T_t = \frac{T_{max} - T_{min}}{2} * \cos\left(\frac{\pi(t-14)}{12}\right) + \left(\frac{T_{max} + T_{min}}{2}\right) \quad (2.28)$$

where, *t* denotes hour of the day at which temperature is being calculated.

Disaggregation of precipitation is much more complicated than temperature because of the unsystematic variability involved at a sub-daily scale. According to Debele et al., 2007, methods used currently for disaggregating daily precipitation either a) uniformly distribute daily rainfall across the day; b) stochastically perform temporal disaggregation of daily data; c) use detailed information from a nearby station to perform disaggregation; and d) perform a multivariate disaggregation by employing a combination of b) and c).

Although observed rainfall is seldom uniform, many hydrologic models distribute daily rainfall uniformly while performing hydrologic simulations. For daily rainfall values (r_d) < 24 mm, hourly precipitation values of 1mm are distributed across first r_d hours and no precipitation is assumed for remaining hours of the day. However, if r_d >=24 mm, rainfall is uniformly distributed across the day.

Performing bias-correction of climate data can change the statistical properties of baseline and future climate data. This also modifies the changes projected by a GCM. For instance, Table 2 and 3 compare the changes projected by raw and bias-corrected GCM datasets for two extreme scenarios selected in Figure 2. It can be seen that the changes in mean as well as mean above 99th percentile are different for bias-corrected (BC-PPT and BC-TMEAN) and uncorrected (UC-PPT and UC-TMEAN) data. Therefore, the selection of extreme GCM-scenario combinations should either be done after the data has been corrected for bias or the methodology chosen for bias-correction should be such that it doesn't impact the changes projected by raw GCM data (Note: Changes projected by raw GCM data are considered accurate as per change factor based statistical

downscaling concept. Therefore, they shouldn't be altered by bias-correction step). On the other hand, downscaling using change factors and weather generator doesn't have significant impact on the changes projected by GCMs. However, the type of change factors used while downscaling GCM data should match with those used while selecting GCM-scenario combinations to ensure that the changes projected by raw GCM data are preserved.

Table 2 Changes in mean projected by raw and bias-corrected GCM scenarios for 2050s

Model	UC-PPT	UC-TMEAN	BC-PPT	BC-TMEAN
IPSL-CM4 (A2)	1.25	60.71	1.58	49.6
CSIRO-MK3.0 (A1B)	2.9	30.21	2.81	21.14

Table 3 Changes in mean above 99th percentile projected by raw and bias-corrected GCM scenarios for 2050s

Model	UC-PPT	UC-TMEAN	BC-PPT	BC-TMEAN
IPSL-CM4 (A2)	0.093	13.66	13.24	15.22
CSIRO-MK3.0 (A1B)	4.57	7.94	4.81	6.23

Also, pre-processing methods are generally reliant on modifying baseline model data with respect to historical observed data, and using same set of transfer functions to modify future model data. In other words, it is assumed that these transfer function relationships will be equally applicable in future timelines as well. Robust methodologies need to be employed which are devoid of such assumptions since they are very unlikely to be true in future.

2.2.3 Generation and analysis of future streamflow projections

Pre-processed data from climate models is used as input in hydrologic models, which generate spatial and temporal distribution of runoff using catchment characteristics. Lumped hydrological models consider entire area under study as a single unit and represent state variables as averaged

values across it. Due to this, lumped models fail to represent catchment scale hydrological processes accurately especially for medium and large catchments (>100 km^2 in area). Distributed models divide the catchment into uniform grid cells and are much more complex than the lumped models. Lack of fine resolution climate data, as required by fully distributed models, makes their calibration process difficult. Defining initial values for hydrological parameters across the catchment grids is difficult for fully distributed hydrological models (Gosling et al., 2011). Semi-distributed models are less complex than distributed models and have a higher spatial resolution of hydrological processes than a lumped model. Here, catchment is distributed to a degree that hydrological properties of the catchment are satisfactorily, if not precisely, simulated in the model. They are generally divided into areas of similar hydrological responses. Hydrological processes within each of these areas are simulated as lumped processes within each sub-catchment and are routed downstream to get flow patterns at the catchment outlet. Semi-distributed and distributed hydrologic models have been found to perform better than the lumped models in simulating hydrological response to climate variables especially for large catchments (Khakbaz et al., 2012).

Continuous hydrological modelling is necessary while estimating peak runoff from a catchment. Unlike event based modelling, it accounts for the state of catchment prior to flood-producing rainfall event, in the modelling procedure. Lack of this antecedent information has been found to produce significantly underestimated peak flows in 45 catchments across the Murray Darling basin (Pathiraja et al., 2012). Similar results are noted when Berthet & Andr (2009) analysed peak flow response of 178 French catchments to event and continuous hydrologic simulations. In their study, Pathiraja et al., (2012) also noted that usage of continuous simulation is even more important in catchments where there is a significant lag between rainfall and runoff peaks.

WATFLOOD hydrological model

WATFLOOD hydrologic model is based on the concept of Grouped Response Units (GRUs), where units of similar hydrological response (or Hydrological Response Units) within the catchment are modelled together to calculate overland flow, interflow and baseflow within the area of study. The resolution of computational grids is chosen keeping in mind the resolution of available meteorological data (generally from numerical weather models or radars) as well as the size of smallest catchment to be modelled. Using remotely sensed land-cover data, these computational grids are sub-divided into sections of unique land-cover classes. The hydrological response from each individual land-cover section is calculated and routed downstream to calculate the runoff response of the catchment under study (Kouwen et al., 1993). For instance, if land-cover image has four classes: A, B, C and D. Hourly runoff is first calculated for each individual class and then, combined together to get total runoff at each grid. Runoff calculated at each grid is routed downstream using physiographic information of the catchment (Figure 4). Figure 5 shows the process by which precipitation and temperature data is utilised in WATFLOOD to generate flows.

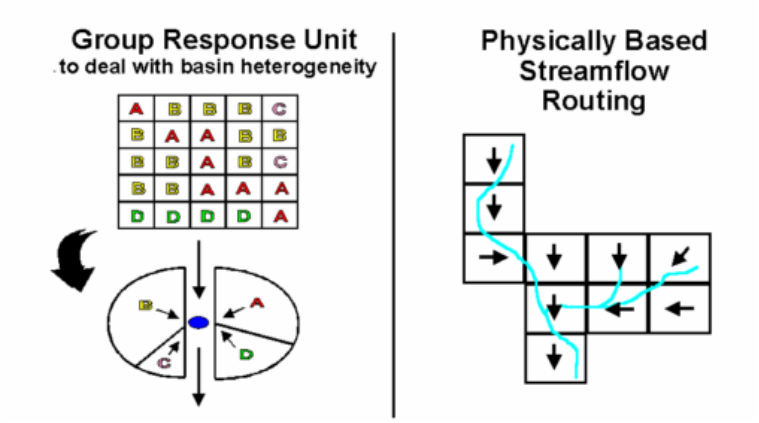

Figure 4 Flow calculation and routing concept used in WATFLOOD

In this setting, hydrological parameters are associated with individual land-cover classes and they remain constant regardless of the composition of different grids existing within the basin area. Therefore, same set of parameters can be used without recalibration in another catchment with similar physiographic characteristics. Also, model need not be recalibrated if land-use within the catchment changes over time. An updated land-use file for the catchment will be sufficient to include changes in the calibrated model making the model extremely suitable for climate change impact studies.

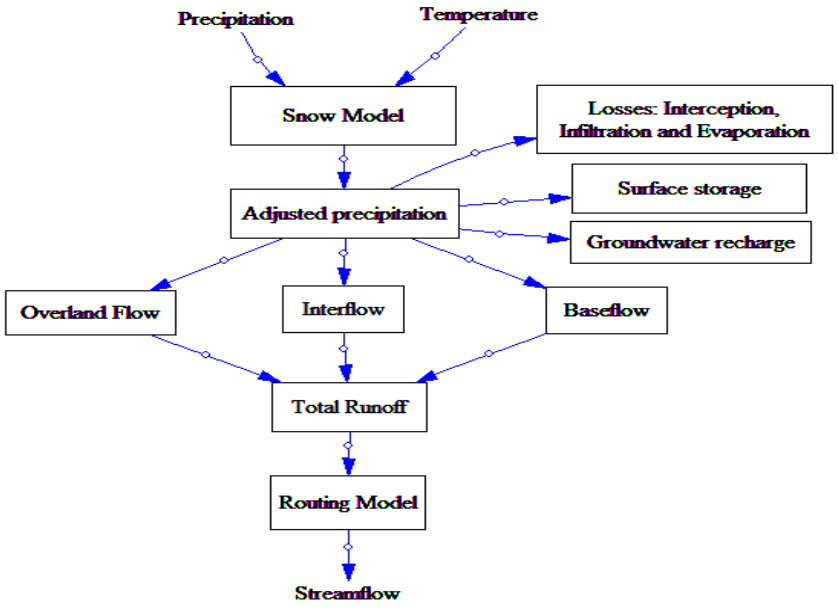

Figure 5 Flowchart of processes involved for streamflow generation in WATFLOOD

Table 4 Description of important input, outputs and subroutines in the WATFLOOD hydrological model

Database	Files	Description
Drainage input	*.map	Watershed map file: has information such as stream elevation, drainage direction, land-cover information etc.
	*.shd	Basin file generated from the map file using programme bsn.exe
	*.par	Parameter file
	*.str	Contains stream gauge and reservoir locations

Meteorological input	*.rag	Contains precipitation gauging station locations and historical records
	*.tag	Contains temperature gauging station locations and historical records
Event input	event.evt	Contains information about the duration for which the simulation will run
Output (imp)	spl.txt	Provides a summary of the modelling parameters, the initial soil moisture, the total precipitation on each element, the runoff at each streamflow gauge station and the errors
	spl.plt	Provides hydrograph plots from the run
	stg.plt	Provides stage plots from the run
	spl.csv	Observed and simulated flow history in *.csv format for import to other programmes
Useful subroutines	radmet.exe	Converts the radar data file into SPL compatible format
	ragmet.exe	Distributes point precipitation data using distance weighting technique
	calmet.exe	Fills-in missing radar data with point precipitation data
	snw.exe	Distributes snow coarse data using distance weighting technique
	moist.exe	Distributes soil moisture data using distance weighting technique
	tmp.exe	Distributes point temperature data using distance weighting technique
	spld.exe	Compiles the model in debug mode with maximum error diagnostics
	splx.exe	Compiles the model with faster speed and lesser error diagnostics
	stats.exe	Calculates a number of statistics for the run

The model is aimed at flood forecasting and long-term hydrologic simulation. It include processes like interception, infiltration, evaporation, snow accumulation and ablation, interflow, recharge, baseflow, overland flow and channel routing (Kouwen et al., 1993). A flowchart depicting the role of these processes in generation of streamflow from climate variables is provided in Figure 5. Hourly precipitation and temperature data is used as input into a snow model and value of adjusted precipitation is obtained. Adjusted precipitation is reduced by losses from interception, infiltration and evaporation. A fraction of water is stored on the surface while some contribute

towards groundwater recharge and baseflow. Remaining water flows overland and combines with baseflow to form total runoff. Generated total runoff is routed downstream to generate streamflow patterns for the catchment under study. A description of major processes involved in WATFLOOD hydrologic model is provided below (Kouwen et al., 1993):

- Interception is calculated using the approach suggested in Linsley et.al. (1949). According to it, total interception is equal to the sum of total canopy storage and the Interception Evaporation (IEP) occurring during a storm event.
- Infiltration processes are accounted for in the model using the Philip formulae (Philip, 1959), which also accounts for surface detention of water. Initially, infiltration rate is high due to large pressure gradient in the surrounding region. The same decreases with time as the gradient decreases.
- Potential Evapo-Transpiration (PET) can be calculated using different methods in WATFLOOD. When radiation (shortwave and longwave) data is available, the Priestly-Taylor equation can be used. When only temperature data is available, Hargreaves equation can be used. If both radiations as well as temperature data are unavailable, PET is estimated using published values from the literature. Estimation of AET involves consideration of water transpired from vegetation and water evaporated from open soils and open water.
- The calculation of snow-melt is performed using degree day approach as described in National Weather Service River Flow Forecast system by Anderson (1973).
- Interflow is the flow of infiltrated water (contributing towards Upper Zone Storage) in the surrounding space. Downward movement of water has been ignored in the model and total interflow is expressed as a linear function of water stored in the upper zone.

- Baseflow is estimated at each sub-division using measured hydrograph at the basin outlet. The magnitude of baseflow is made to recede with time using a recession constant. However, the contribution of baseflow has been found to be negligible with respect to overland flow during the flooding events.
- Overland flow is the component of flow exceeding the depression storage. It is estimated in the model using a modified form of manning's formula. Total runoff is calculated by adding up overland flow contributions from different land-use classes to the baseflow.
- Routing of overland flow across the channel cross-section is carried out using simple storage-routing technique. Relationship between overland flow and channel storage is expressed using Manning's formula.

The WATFLOOD is a compilation of FORTRAN code subroutines and can be run on DOS and UNIX platforms. Its main advantage is that it is very fast, robust, can run with minimal (precipitation and temperature) inputs and its transferability to other watersheds without recalibration. Although model runs are performed on hourly temporal scale, meteorological inputs (except temperature) can be provided in daily time steps as well. If provided in daily timesteps, climate data is temporally disaggregated internally using standard climate variable disaggregating procedures and are used to generate streamflow response. Table 4 provides a list of major input files, output files and set of programmes that define WATFLOOD with their short descriptions.

Statistical analysis

Flood frequency analysis is performed to develop relationships between flood magnitude and flood recurrence interval. The same is achieved by performing a statistical analysis on time-series of peak flows. There are two methods of extracting peak flow data from a discharge series,

namely Annual Maximum (AM) and Peak Over Threshold (POT) method. In AM method, yearly maximum discharge values are selected while in POT method, discharge events larger than a specified threshold are considered for analysis. Major limitation of AM method is that the values extracted may not be representative of actual peaks in the entire discharge series. For example, the second largest discharge in a high-flow year may be higher than peaks of many other low-flow years in the discharge series, but will be ignored by the AM method since only one (maximum) value is selected per year. Another limitation is that sample size of peak flows obtained from the AM method is small (equal to the number of years of discharge series data) and hence, reliable statistical inferences are hard to be drawn from it. POT method, on the other hand, overcomes these limitations and is extremely useful especially when the available discharge series is short.

The flood magnitude-return period relationship for POT model is:

$$1 - F(Q_T | Q_T > q_0) = \frac{1}{\lambda T} \tag{2.29}$$

where *F()* is the cumulative distribution of the discharges exceeding the threshold q_0, and λ is the number of peaks selected per year.

While selecting values for analysis using POT method, it should be ensured that they are independent and don't belong to the recession curves of previous flow peaks. Further, selection of an appropriate threshold value is of utmost importance. Although no strict rules are existent for selection of this threshold, guidelines for doing so have been summarised in Lang & Bobe, 1999. They identified three criteria to be considered while selecting a threshold value. These are related to a) "mean number of over-threshold events", b) "mean exceedence of threshold" and c) "dispersion index" obtained from the selected values. Mean exceedence over threshold criterion is

based on the objective of stabilisation of POT distribution parameters. It has been found that choosing a threshold value within an interval where a linear relationship between threshold value and mean exceedence is observed, increases the stability of distribution parameters. Hence, recommendations have been made to locate this range and then test different threshold values within this range for their dispersion characteristics. First and third criteria aim to select peaks following characteristics of a Poisson's process or in other words, are randomly distributed over time. To account for it, a value of λ>2 or 3 is recommended for usage.

Flow peaks crossing a threshold can be fitted using a Generalised Pareto Distribution (GPD). The cumulative distribution function *F(x)* for the GPD can be given by the following equations:

$$F(x) = 1 - (1 - k\frac{(q-q_0)}{\beta})^{1/k} \qquad \text{if } k \neq 0 \qquad (2.30)$$

$$F(x) = 1 - exp(-\frac{(q-q_0)}{\beta}) \qquad \text{if } k=0 \qquad (2.31)$$

where, q_0 is the threshold, β is a scale parameter and k is shape parameter. When $k=0$, it represents an exponential distribution.

The inverse form of the GPD is:

$$q(F) = q_0 + \frac{\beta}{k}[1 - (1 - f)^k] \qquad \text{if } k \neq 0 \qquad (2.32)$$

$$q(F) = q_0 - \beta \ln[1 - F] \qquad \text{if } k = 0 \qquad (2.33)$$

Method of L-moments is most frequently used for parameter estimation in hydrological studies. This parameter estimation method has been found to perform better than other traditional methods like method of moments and maximum likelihood, particularly when the sample size is

small (Chin, D.A., 2006). The method has also been found robust against outliers present in datasets (Hosking, 1989). In this method, L-moments are expressed as the linear combinations of Probability Weighted Moments (PWM). The expressions for calculating PWMs and L-moments are summarised in Table 5.

As mentioned in Das and Simonovic, (2012), two different approaches can be taken while estimating parameters of GPD using L-moments.

i. An initial value of threshold q_0 is fixed and data values crossing it are picked from the data sample (say *M* nos.). In this case, only two parameters β and *k* need to be estimated.

ii. An initial value of λ is fixed and a total $(\lambda \times N)$ number of values are picked from the entire timeseries. Peak *M* flows are then selected out of those values and parameters q_0, β and *k* are estimated.

For *(i)* parameters β and *k* are given by Hosking and Wallis, (1997)

$$k = ((l_1 - q_0)/l_2) - 2 \tag{2.34}$$

$$\beta = (1 + k)(l_1 - q_0) \tag{2.35}$$

For (ii) parameters q_0, β and *k* are given by Hosking and Wallis, (1997)

$$k = (l_1 - 3t_3)/(1 + t_3) \tag{2.36}$$

$$\beta = (1 + k)(2 + k)l_2 \tag{2.37}$$

$$q_0 = l_1 - (2 + k)l_2 \tag{2.38}$$

where $l_1$is the 1st L-moment, l_2 is the 2nd L-moment and $t_3$is L-skewness.

Table 5 Expressions for calculation of L-moments and L-moment ratios (Chin, D.A.,2006)

Population quantile	**Sample estimates**
1st PWM (b_0)	$\frac{1}{N}\sum_{i=1}^{N} x_i$
2nd PWM (b_1)	$\frac{1}{N(N-1)}\sum_{i=2}^{N}(i-1)x_i$
3rd PWM (b_2)	$\frac{1}{N(N-1)(N-2)}\sum_{i=3}^{N}(i-1)(i-2)x_i$
4th PWM (b_3)	$\frac{1}{N(N-1)(N-2)(N-3)}\sum_{i=4}^{N}(i-1)(i-2)(i-3)x_i$
1st L-moment (L1)	b_0
2nd L-moment (L2)	$2b_1-b_0$
3rd L-moment (L3)	$6b_2-6b_1+b_0$
4th L-moment (L4)	$20b_3-30b_2+12b_1-b_0$
L-Coefficient of Variation	*L2/L1*
L-Skewness	*L3/L2*
L-Kurtosis	*L4/L2*

(Note: Sampling data needs to be arranged in ascending order before calculating the values of PWMs).

3 CASE STUDY: GRAND RIVER AT BRANTFORD CATCHMENT

Methodology discussed in Section 2 is applied to the Grand River catchment to estimate changes in the probability of occurrence of future flood extremes.

3.1 Introduction of the basin

Grand River has the largest drainage area among all southern Ontario rivers. It originates in Dundalk and Grand valley region (525 masl) and flows 128 km southwards to drain into Lake Erie (100 masl) at Port Maitland (Figure 6). It crosses urban centres of Kitchener, Waterloo, Cambridge, Guelph etc. on its way to the summit (Stadnyk-Falcone, 2008).

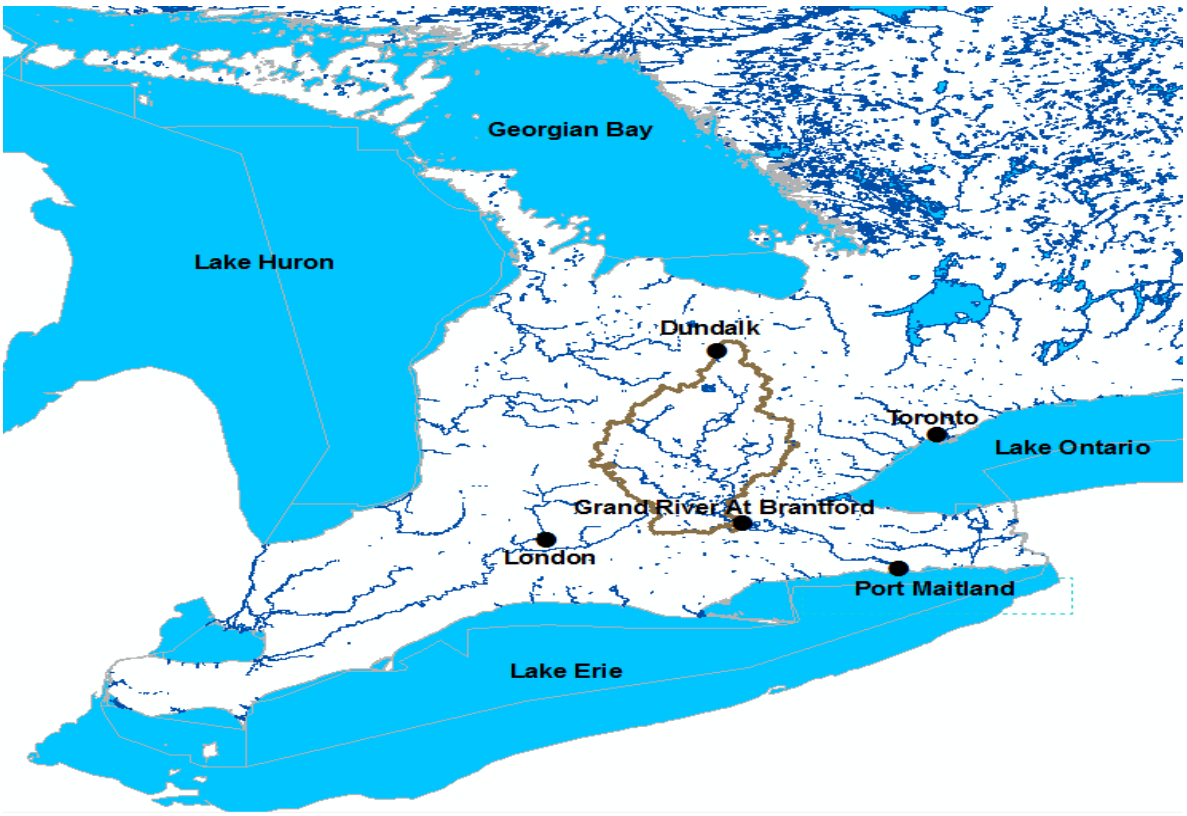

Figure 6 Geographic settings of the Grand River at Brantford

The Grand River watershed is home for more than 787,000 people, who depend on the river for fulfilling their needs of water for agriculture, transportation, drinking and power generation. A major section of the population resides in the central regions of the watershed with northern and southern regions generally used for agricultural purposes (Boyd etal., 2009).

Based on the geologic setting, Grand River watershed can be roughly classified into three sections of upper Grand watershed (flat with poorly drained clayey soil), central Grand watershed (steep with well-drained soil) and lower Grand watershed (flat and low-lying with a mix of silty and clayey soil) (Grand River Conservation Authority, 2005). Catchment of Grand River at Brantford, with an area of 5,210 km^2 roughly encompasses the upper and central Grand River catchments. There is a heterogeneous land-cover spread throughout the catchment. A major portion of the catchment is used for agricultural purposes. Northern regions are abundant with surface water and moraines due to the presence of clayey soil and thus, contribute heavily towards total surface-runoff from the catchment (Boyd et al., 2009). Big urban centres Kitchener, Waterloo, Cambridge etc. are present in the central and south-eastern regions of the catchment promoting urban land-use in the area. Southern portion of the catchment is dominated by vegetation and forests (see Figure 7).

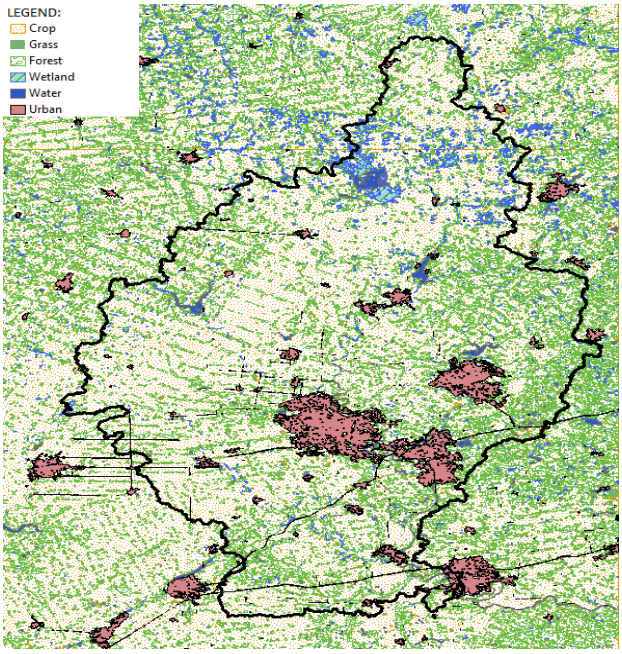

Figure 7 Land-use classification of the Grand River at Brantford

Average annual precipitation across the catchment is approximately 900 mm though it shows significant spatial and temporal variations. For instance, average annual precipitation for gauging stations Monticello, Elmira and Falkland, located in the northern, central and southern regions of the catchment is 960 mm, 750 mm and 710 mm respectively. Significant temporal variations in precipitation patterns are observed as well. A major fraction of annual precipitation occurs in the summer months of April to August and relatively smaller precipitation is experienced in other months.

The annual average flow at Brantford (for the duration 1960-2000) is 57.83 m^3/s. Monthly variations in flow patterns are also noted. As shown in Figure 8, peak discharges are observed in March and April and low flows are observed in the summer months. Further, relatively higher values of discharges are noted in all the winter months. These observations suggest higher

possibilities of snowmelt runoff, ice on flood or ice jam floods in the catchment than the storm rainfall floods.

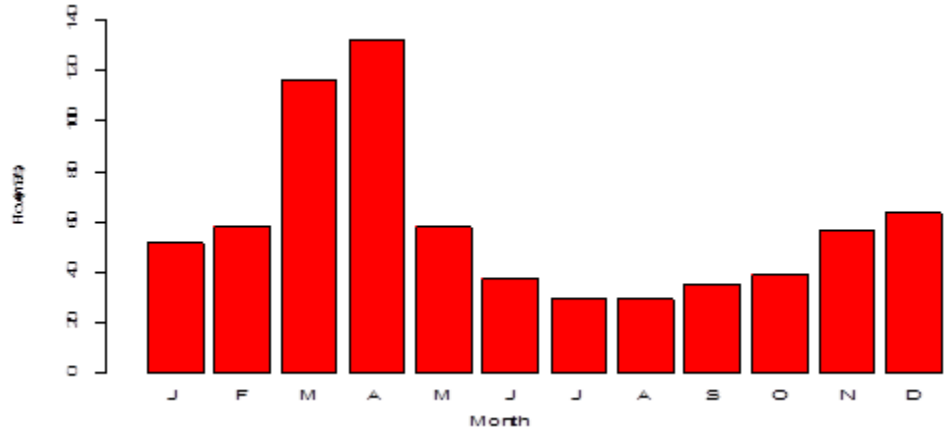

Figure 8 Monthly variability of average flows recorded at Brantford

Flow is regulated at several locations along the Grand River to ensure continuous, necessary and sufficient supply of water for the communities living downstream. Luther dam, Damascus dam, Conestogo dam, Woolwich dam, Laurel dam, Shand dam, Guelph dam and Shade's Mills dam are the major dams existing within the catchment. In addition to them, a series of dykes also protect parts of Kitchener, Cambridge and Brantford from high flows. However, with continued deforestation, growing urban population and changing climate, runoff patterns within the catchment are expected to change in the future. Authorities will face the challenge to frame appropriate water management policies for managing flow extremes within the catchment (Farwell et al., 2008).

3.2 Data collection

A suit of different climate datasets are collected from several sources for this study. Datasets and their respective sources are discussed below.

3.2.1 Observed daily climate data

Historical observed precipitation and temperature (maximum, minimum and mean) data for the period 1960-2000 is collected from the National Climate Data and Information Archive (NCDIA) using Canadian Daily Climate Data (CDCD) software at 52 precipitation and temperature gauging stations falling within the Grand river catchment and having data within the period 1961-2000. A list of gauging stations at which climate data is collected, is provided in Appendix B. The CDCD software can be used to download observed daily temperature, precipitation and snow-on-the-ground data, and is downloadable for free from the NCDIA website.

3.2.2 Daily historical and future GCM data

Programme for Climate Model Diagnosis and Inter-comparison (PCMDI) archive offers a collection of historical and future daily, monthly and yearly climate datasets for all climate models mentioned in IPCC, (2007) to facilitate diagnosis and inter-comparison between them (Meehl et al., 2007). These multi-model datasets are the product of the Coupled Model Inter-comparison Project phase 3 (CMIP3) of the World Climate Research Programme (WCRP).

Gridded historical GCM data corresponding to *Climate of the Twentieth Century* simulations are downloaded for fifteen climate models mentioned in IPCC, (2007). A list of these fifteen climate models with specifications is provided in Appendix C. Future GCM data corresponding to selected model-scenario combinations is also downloaded from the PCMDI

archive. These datasets are available in NetCDF (*.nc) file format and are accessed and analysed using R statistical programming language (R Development Core Team, 2008).

3.2.3 Historical observed hourly precipitation data

Hourly precipitation datasets for the duration 1961-2000 are obtained from the Grand River Conservation Authority (GRCA) at 21 stations located across the Grand River catchment. A list of these stations has been attached in Appendix D.

3.2.4 Historical observed daily streamflow data

Historical observed stream-flow data is collected at four discharge stations: Brantford, Galt, West Montrose and Shand dams located within the Grand River basin. These discharge stations are spread out widely across the catchment and have historical discharge data available for the period 1993-2000 (period chosen for hydrological model validation). Figure 9 shows the spatial distribution of discharge stations across Grand River at Brantford.

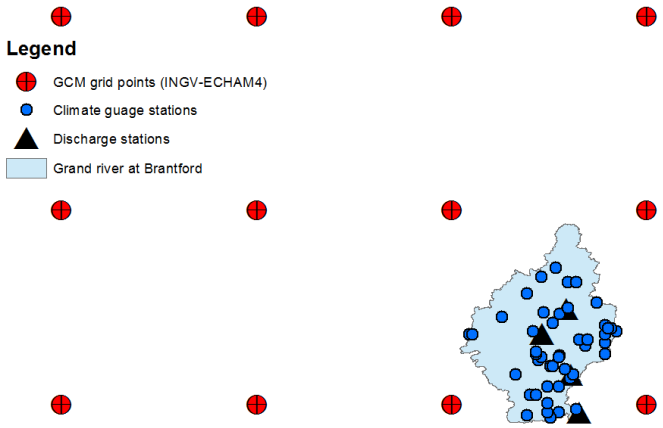

Figure 9 Spatial distribution of climate gauging and discharge stations across Grand River at Brantford. Grid data points are also plotted for a sample GCM (INGV-ECHAM4)

3.2.5 Historical reanalysis daily climate data

Reanalysis datasets are produced by combining a numerical model, capable of simulating one or more aspects of the Earth's system, with climate observations made from several sources as ships, satellites, ground stations, radiosonde databases (RAOBS) and radars. They provide reliable climate data that extends from Earth's surface to the stratosphere. NCEP/NCAR I provides gridded reanalysis data throughout the world, from 1948 till present, on a 2.5ºx2.5º and 2ºx2º Gaussian spatial scale (Kalnay et al.,1996). NARR reanalysis is a relatively recent effort to produce high resolution reanalysis datasets (with a spatial resolution of 32 km) for North America (Mesinger et al., 2006). Inputs of both these reanalysis products are similar, but NARR output is obtained by using a lower resolution climate model and hence, is more accurate. Datasets from both the projects are used in this analysis. Wherever possible, NARR datasets are preferred over NCEP/NCAR I for their high accuracy. However, since NARR data is only available since 1979, NCEP/NCAR I datasets are used for period (1960-1979.

3.2.6 Catchment boundary for Grand River at Brantford discharge station

Catchment boundary for Grand River at Brantford discharge gauging station is obtained from the Environment Canada (shown in Figure 9).

3.2.7 Historical reservoir release data

Daily historical reservoir release datasets for reservoirs at Conestoga, Luther, Shades, Guelph, Laurel, Woolwich and Shand dam for the duration 1984-present is provided by the Grand River Conservation Authority (GRCA). Hourly release data for the year 2012 at these reservoirs is also provided by the GRCA.

3.3 Analysis

Keeping in mind the availability of data, fifteen climate models and eighty-six scenarios associated with them are selected for analysis. Gridded daily historical climate model data corresponding to selected GCM-scenario combinations is spatially interpolated at 52 gauging stations lying within the Grand River catchment using Inverse Distance Square method. Further, intermittent historical observed data is filled-in using spatially interpolated reanalysis data to produce a continuous series of precipitation and temperature over the period of study (1961-2000). NCEP/NCAR daily precipitation data are available for the duration 1948-present while NARR precipitation data are available from 1979-present. Owing to their higher resolution, NARR datasets are preferred over their NCEP/NCAR counterparts. Maximum and minimum temperature data is available only for the NCEP/NCAR data product. Therefore, daily NCEP/NCAR gridded reanalysis datasets are used to fill in gaps in the observed t_{mean}, t_{max} and t_{min} data for the entire period of study. For precipitation, interpolated daily NCEP/NCAR and NARR reanalysis precipitation datasets are used to fill-in the missing observed data for the period 1961 to 1978 and 1979-2000 respectively.

Using interpolated baseline GCM data and filled-in observed historical data (for the duration 1961-2000), monthly bias-correction transfer functions are established at each gauging station. Obtained transfer functions are used to bias-correct historical and future GCM data at all 52 gauging stations using statistical bias correction approach. For bias-correction of GCM precipitation data, Piani et al., (2010) provided reasonable limits ($a<0$ and $1/5<b<5$) for linear transfer function parameters ‘a’ and ‘b’. As explained before, exponential transfer functions are used in case these thresholds are exceeded.

Monthly bias correction transfer functions obtained at each gauging station are disaggregated into daily timesteps using methodology explained before. Daily transfer functions are used to modify historical and future GCM data to obtain bias-corrected historical and future precipitation and temperature data.

Historically observed and bias-corrected historical and future GCM data are used together to downscale future climate projected by GCMs. Multiple additive and multiplicative CFs are used to generate future scaled temperature and precipitation data respectively. Total number of bins is chosen to be 100 and variable distribution is kept uniform across them. Generated future scaled data is imported in the M3EB weather generator to generate twenty different sets of future downscaled climate data for each GCM-scenario combination selected for analysis.

Synthetic realisations corresponding to each model obtained from the weather generator are used to select variable combinations most likely to cause hydro-climatic extremes in the future. This is done by selecting extreme scenarios from scatter-plots prepared at each gauging station lying within the catchment. Figure 10 shows the selected cold-dry and hot-humid extreme scenarios at Apps Mills gauging station.

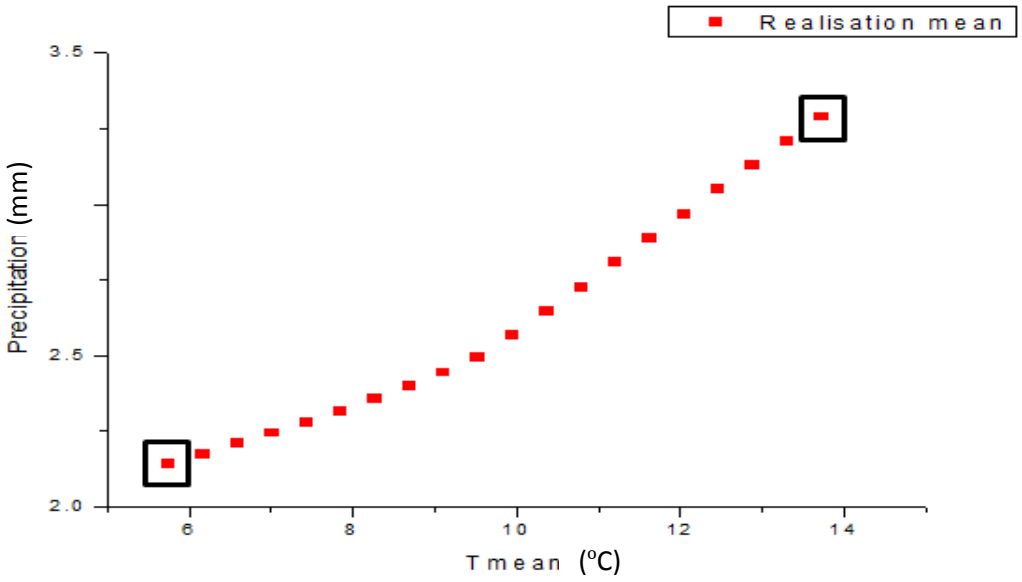

Figure 10 Extreme scenario cold-dry and hot-humid selected from twenty realisations obtained for *csiro-mk3.0(A1B), run1, 2050s* at Apps Mills climate gauging station

Since a significant portion of flooding in the Grand river basin occurs due to snow accumulation and melt (Boyd et al., 2000), continuous hydrological modelling is performed to generate streamflows from the selected extreme precipitation-temperature scenarios. A semi-distributed model WATFLOOD is used and future streamflows are generated for 2050s and 2090s. This model has been found to simulate the hydrologic behaviour reasonably well for the catchment under study as well as for many other regions across the globe (Bingeman et al., 2006; Kouwen et al., 1993).

The model calibrated for Grand River basin for the period 2000-2005 is obtained from Dr. Nicholas Kouwen (Professor Emeritus, University of Waterloo). Provided model is validated on the Grand River at Brantford catchment for the period 1993-2000 and satisfactory validation results are obtained at four discharge stations Brantford, Galt, West Montrose and Shand dam.

Coefficient of determination (R-square) values for modeled and observed flow series obtained at four discharge stations lying within the catchment are listed in Table 6. Of note is that this discharge validation is obtained considering historical precipitation and temperature data filled-in using spatially interpolated reanalysis data. Also, land-use change which plays a crucial role in WATFLOOD model, has been ignored between calibration and validation time-periods. Once validated, the hydrologic model is used to generate flow series for future timelines. Land-use change is ignored (and will be addressed in future research) and releases at Shand, Conestogo, Shades, Luther, Laurel, Woolwich and Guelph reservoirs are held constant to the most recent releases (taken as 2012).

Table 6 Coefficient of determination values for daily and monthly historical flow series simulated by the hydrologic model

Discharge stations	Daily series	Monthly series
Brantford	0.700	0.800
Galt	0.767	0.900
West Montrose	0.832	0.921
Shand dam	0.952	0.995

Historical observed and generated future flow-series are used to obtain flood magnitude and return period relationships. In this study, POT method is employed to select flow peaks. Selection of independent peak discharge values is made using the software WETSPRO (Willems, 2009). The selection of independent flow peaks in WETSPRO is made using the following three criteria:

- Time between the two peaks should be greater than the recession constant *k* (time in which flow becomes lower than 37% of its peak value).
- Minimum discharge between the two peaks should be less than a fraction *f* of the peak discharge.

- Peak discharge should be greater than the threshold discharge value q_{lim}.

Values of parameters “k” and “f” have been chosen as 10 and 0.37 respectively. A reasonable estimate of threshold q_{lim} is made for each flow-series following the guidelines mentioned before. Mean exceedence above threshold vs. threshold value plots are prepared for each flow-series to be analysed and the range of threshold domain is estimated. Plots generated to estimate the threshold domain for historically observed flows at Brantford is provided in Figure 11. To prepare these plots, mean exceedence value of flowseries crossing a particular threshold value is calculated and plotted against the threshold values. The process is repeated for several threshold values selected within the variable range. Values obtained for mean exceedence above threshold are plotted against mean threshold and region where a linear relationship exists between them is identified. An appropriate value of threshold is then decided within the threshold domain, so that total number of POT selections are above 3N (here, N denotes the number of years of available data) to satisfy the Poisson process criterion or for selected values to be randomly distributed over distribution space.

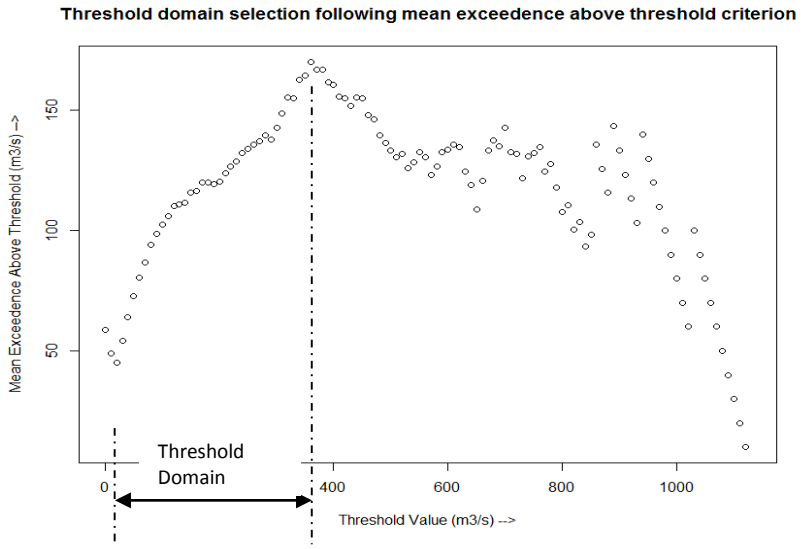

Figure 11 Estimation of threshold domain for historically observed flows at Brantford

Selected flow peaks are used to fit a GPD and associated parameters are estimated using L-moments method. Flow quantiles corresponding to 2-year, 5-year, 10-year, 25-year, and 100-year return period floods are calculated. Also, return-period and flow quantile relationship is established.

4 RESULTS AND DISCUSSION

Statistical bias correction approach is found reasonably effective in correcting bias associated with all moments of the GCM data. The effectiveness of methodology is displayed in Figures 12 and 13 where a comparison between Probability Distribution Functions of raw and bias-corrected GCM data is made. It can be seen that the overlap between observed and GCM data increased on bias-correction of precipitation as well as temperature data. Similar results are obtained for other GCMs considered in this analysis at different gauging stations across Grand River catchment.

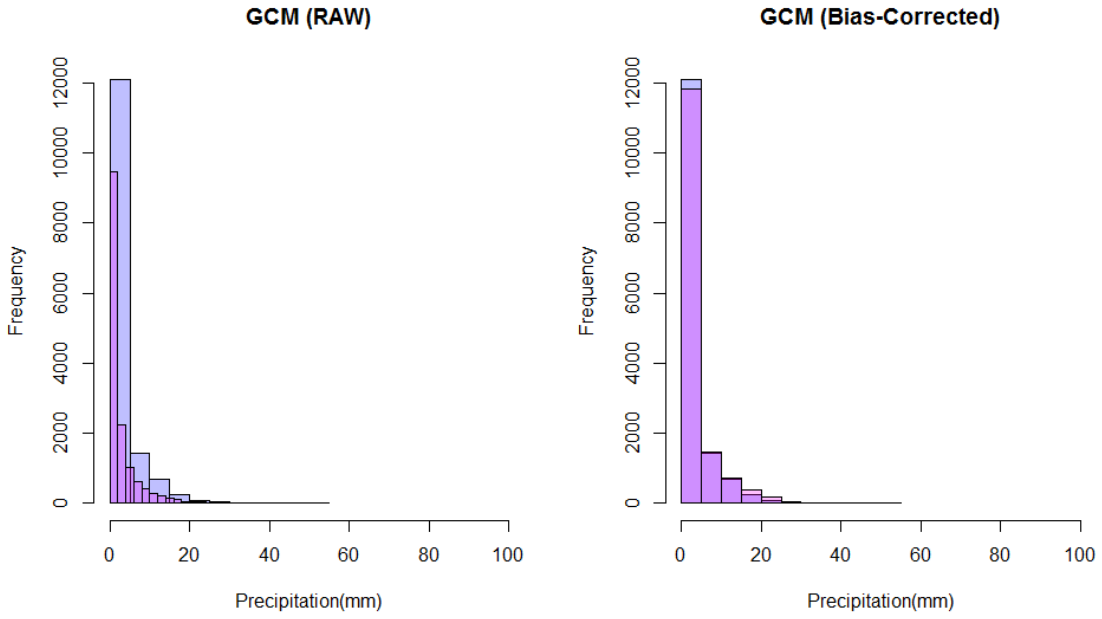

Figure 12 Comparison of bin frequency distributions of observed, raw GCM and bias-corrected GCM precipitation data at gauging station appsmills for giss-aom (Run 1) climate model. Blue colour represents the observed data, pink represents model data and purple represents an overlap between the two.

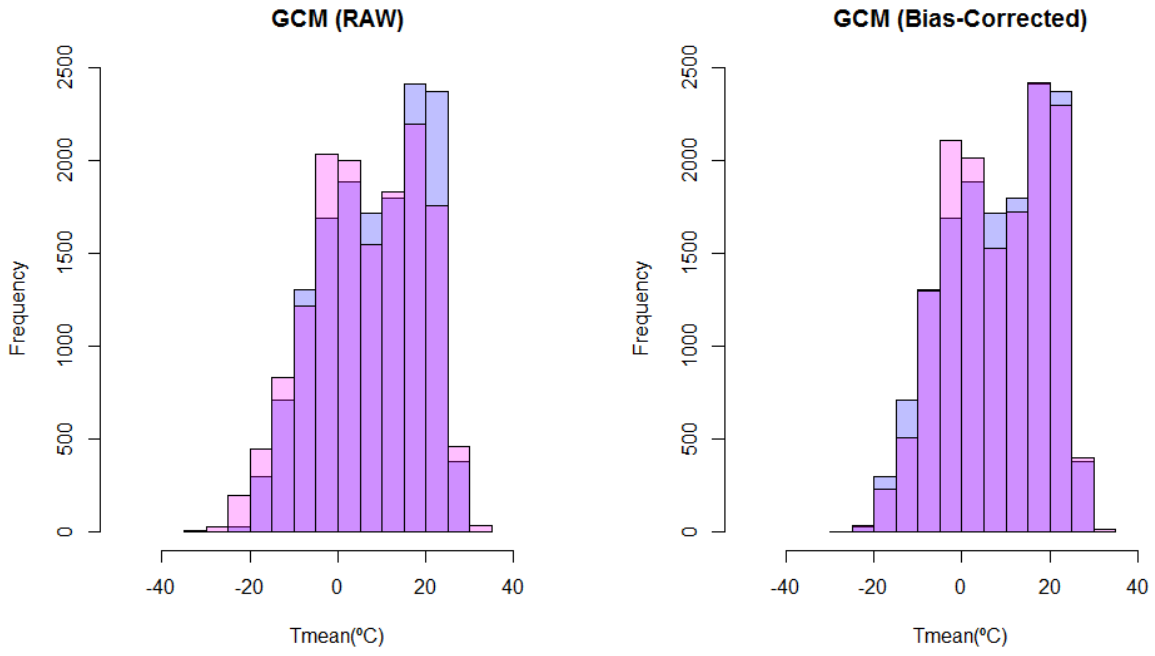

Figure 13 Comparison of bin frequency distributions of observed, raw GCM and bias-corrected GCM T_{mean} data at gauging station appsmills for giss-aom (Run 1) climate model. Blue colour represents the observed data, pink represents model data and purple represents an overlap between the two.

Significant changes in precipitation and temperature regimes have been projected across the catchment. In Figure 14, GCM averaged changes projected in precipitation and temperature means and extremes for timeline 2046-2065 have been summarised. It can be noted that an increase in the intensity of mean and extreme precipitation and temperature events is projected across the catchment. It can also be noted that changes projected for precipitation and temperature extremes are more variable than those projected for means. This also justifies the need for usage of multiple change factors to capture changes in entire distributions of climate data.

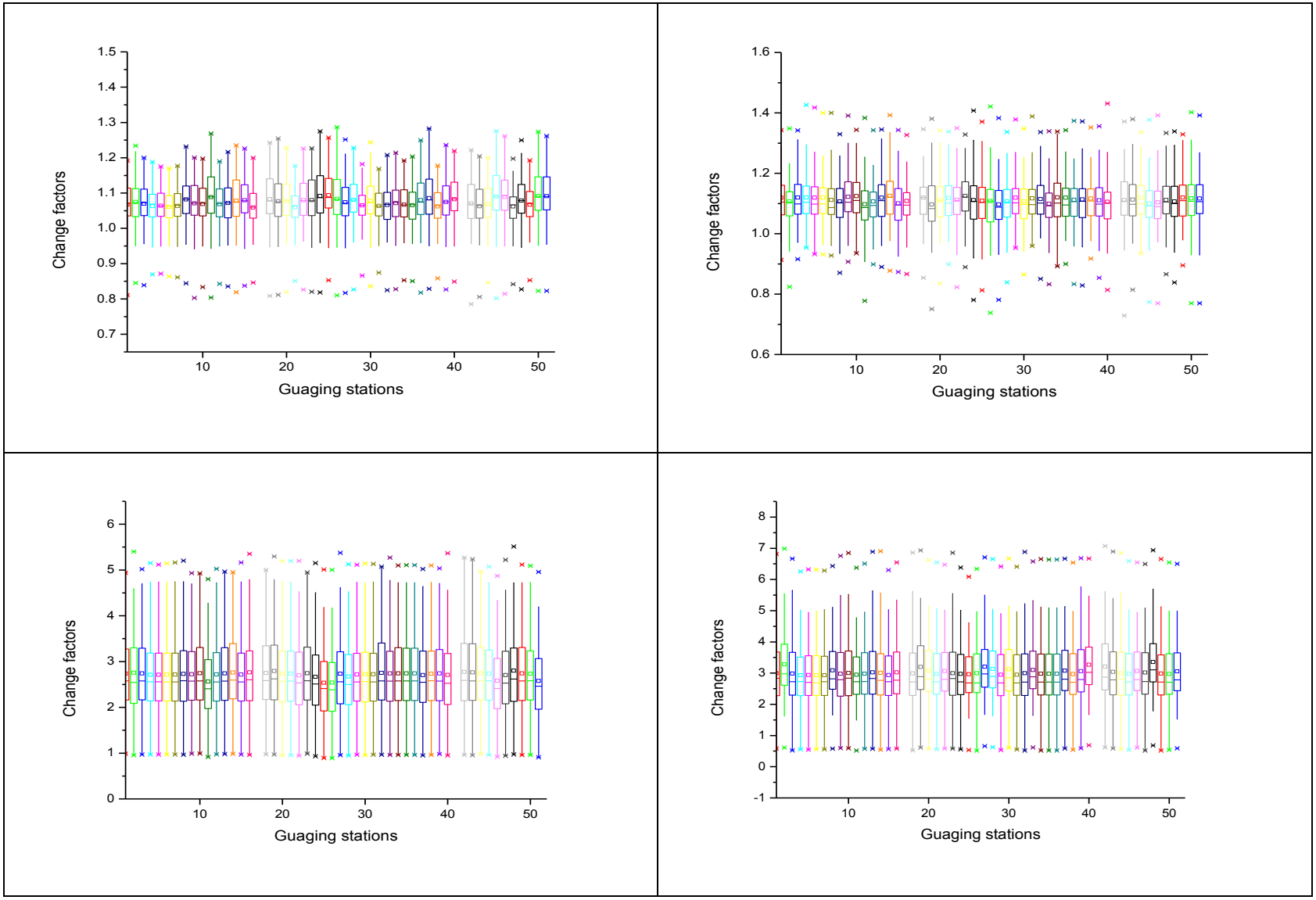

Figure 14 Change factors obtained for precipitation and T_{mean} for 2050s calculated at 52 gauging stations lying within the catchment. Clockwise from top: precipitation means, precipitation above 99th percentile mean, temperature above 99th percentile mean, temperature mean

It has been found that mean changes in precipitation across the catchment range from around +6% to +9.5% for 2050s and +8.5% to +13.6% for 2090s. Average extreme precipitation changes range from +9.7% to +12.5% for 2050s and +13.1% to +17.4% for 2090s. Similar trends are projected in case of temperature as well. Average changes in T_{mean} range from +2.54 ºC to +2.8 ºC for 2050s and +3.86 ºC to +4.27 ºC for 2090s. Average changes (across GCMs) in temperature extremes range from around +2.93 ºC to +3.35 ºC for 2050s and +4.25 ºC to +4.85 ºC for 2090s.

Table 7 Percent change in flow quantiles of 2-year, 5-year, 10-year, 25-year and 100-year extreme event projected in accordance with two hydro-climatic extreme scenarios: "Cold and Dry" & "Hot and Humid"

Scenario	Timelines	Change	2-year	5-year	10-year	25-year	100-year
Cold and Dry	2050s	Max	75.12	43.30	33.36	27.71	24.67
		Min	12.49	-5.97	-15.17	-23.14	-30.01
	2090s	Max	86.03	54.32	43.85	41.59	42.45
		Min	14.22	-2.24	-6.64	-13.38	-18.79
Hot and Humid	2050s	Max	85.62	46.93	32.28	20.02	8.88
		Min	6.94	-9.86	-15.83	-20.68	-25.43
	2090s	Max	100.89	58.43	42.94	30.23	18.83
		Min	23.19	4.14	-5.73	-15.36	-24.06

A subsequent increment in flows is observed at Brantford as summarised in Table 7. It is found that flow quantiles corresponding to extreme flow events increase in future although a wide range of flows may exist. For low return period events, consistent increase in flow quantiles is projected for all scenarios considered. However, for higher return period events, considerable range is evident in the projections. Therefore, sign of change can't be inferred with certainty.

Of the two hydro-climatic scenarios considered, "Hot and Humid" scenario projects higher flows for low return period events while "Cold and Dry" scenario projects higher flows for higher return period events (Table 7). This highlights the role of snowmelt in causing extreme flow events in the catchment. The possibilities of coupling between an intensified hydrological cycle as well

as enhanced snow-cover may result in unprecedented changes in flow patterns in future. It also reiterates the importance of considering all possible hydro-climatic extreme scenarios into analysis. Conversely, return periods of extreme events are expected to decrease in future but again an array of changes are possible in future. Figure 15 highlights this by comparing future projected extreme flow statistics with respect to baseline statistics. Cumulative probability vs. flow and flow vs. return period curves have been used to make the comparisons. Uncertainty associated with future extreme events is particularly evident in each of the results.

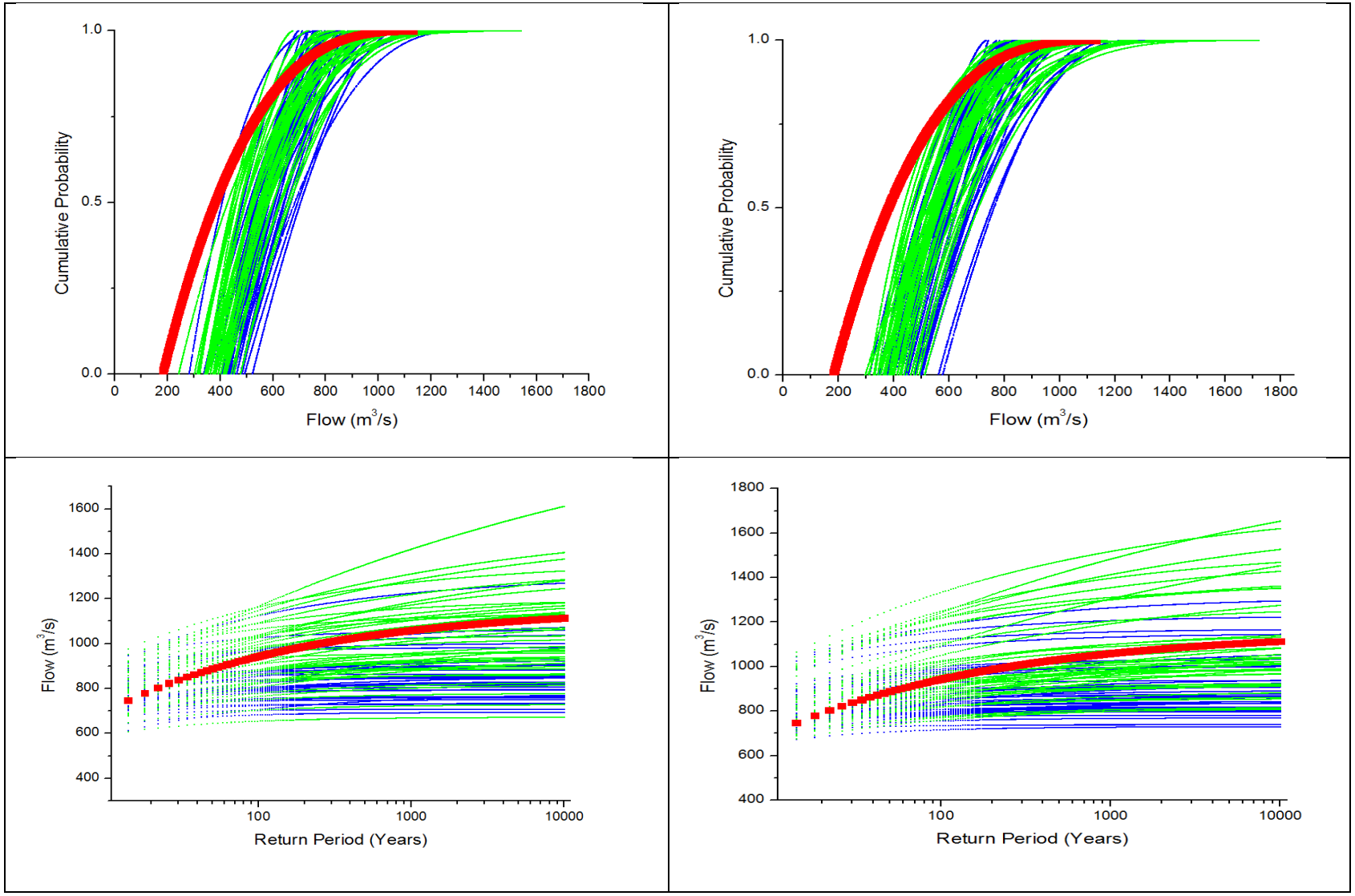

Figure 15 Flow vs. probability and return-period vs. flow curves for projected 2050s and 2090s flows at Brantford. Projections in green correspond to cold-dry scenarios while those in blue correspond to hot-humid scenario. Historical observed flows are marked in bold red. Clockwise from top: flow vs. probability (2050s), flow vs. probability (2090s), return-period vs. flow (2050s), return-period vs. flow (2090s).

5 CONCLUSIONS

Following conclusions can be made based on the previous discussion of methodology followed by climate change impact analysis, and from the results obtained from the Grand River at Brantford case study. .

5.1 Methodology for climate change impact analysis

- Inclusion of every possible GCM-scenario combination in the analysis is important to account for the uncertainty associated with future climate projections. In this respect, availability of continuous climate data for different future scenarios and climate variables is important.
- Plotting methodologies like scatter-plot and percentile-plot are useful if selection of a few GCM-scenario combinations is to be made out of them. This process of scenario selection reduces the amount of work involved in the analysis as well as is helpful in encompassing the uncertainty involved with future projections.
- If selections are being made, same should be done after correcting climate data for bias (in case bias correction step is being performed).
- Pre-processing steps do change climate data statistics, which in turn impact the changes projected by GCMs for future. Therefore, methodology chosen to pre-process model data should be consistent and care should be taken to keep the projected changes by model data intact.

- Suitable spatial, temporal and distributional scale should be selected for different steps in the analysis. It is important to consider all hydro-climatic extreme scenarios while generating future flows so that uncertainty associated is encompassed.
- Semi-distributed or distributed hydrologic models are preferred over lumped models while performing hydrologic modelling. Also, continuous hydrological modeling should be employed. There is a need to account for non-stationarity while performing hydrological modeling step. There is a need to account for changes in land-use among many other changes that may have an impact on future flow extremes.
- Peak Over Threshold (POT) method can be used to select flow extremes for performing statistical analysis. Selection of threshold value should be made for historical as well each future scenario data using "mean exceedence over threshold" vs. "threshold value" graphs and also maintaining the independency of selected peaks.

5.2 The Grand River at Brantford case study

- Intensity of mean and extreme precipitation and temperature events is going to increase in future across the catchment. Consistent increases are projected by all scenarios considered in the analysis for both future timelines.
- Consequent changes in frequencies of 2-year, 5-year, 10-year, 25-year and 100-year return period events are also projected for future. A wide range of changes are projected by the scenarios considered in this study. This array of climate projections should be utilised judiciously by the decision-makers depending on the type of usage of the result.

6 REFERENCES

Alexander, L. V., Zhang, X., Peterson, T. C., Caesar, J., Gleason, B., Klein Tank, a. M. G., Haylock, M., et al. (2006). Global observed changes in daily climate extremes of temperature and precipitation. *Journal of Geophysical Research*, *111*(D5), D05109. doi:10.1029/2005JD006290

Anderson, E.A. 1973. National Weather Service River Forecast System-Snow Accumulation and Ablation Model. National Oceanographic and Atmospheric Administration, Silver Springs, Md., Tech. Memo NWS_HYDRO-17

Anandhi, A., Frei, A., Pierson, D. C., Schneiderman, E. M., Zion, M. S., Lounsbury, D., & Matonse, A. H. (2011). Examination of change factor methodologies for climate change impact assessment. *Water Resources Research*, *47*(3), W03501. doi:10.1029/2010WR009104

Baldwin, D. J. B., Desloges, J. R., and Band, L. E.: 2000, 'Physical Geography of Ontario', in Perera, A. H., Euler, D. E., and Thompson, I. D. (eds.), *Ecology of a Managed Terrestrial Landscape: Patterns and Processes of Forest Landscapes in Ontario*, University of British Columbia Press, Vancouver, B. C., pp. 141–162

Barrow E, B. Maxwell and P. Gachon (Eds), 2004. Climate Variability and Change in Canada: Past, Present and Future, ACSD Science Assessment Series No. 2, Meteorological Service of Canada, Environment Canada, Toronto, Ontario, 114p

Barrow, E., & Yu, G. (2005). CLIMATE SCENARIOS FOR ALBERTA A Report Prepared for the Prairie Adaptation Research Collaborative (PARC) in co-operation with Alberta Environment, (May), 1–73.

Berthet, L., Andréassian, V., Perrin, C., and Javelle, P.: How crucial is it to account for the Antecedent Moisture Conditions in flood forecasting? Comparison of event-based and continuous approaches on 178 catchments, Hydrol. Earth Syst. Sci. Discuss., 6, 1707-1736, doi:10.5194/hessd-6-1707-2009, 2009

Bingeman, A. K., Kouwen, N., Asce, M., & Soulis, E. D. (2006). Validation of the Hydrological Processes in a Hydrological Model, (October), 451–463.

Boyd, D., Cooke, S., Yerex, W., "Exploring Grand-Erie connections: Flow, quality and ecology", 9th Annual Grand River Watershed Water Forum. 18 September 2009. www.grandriver.ca/WaterForum/Boyd09.pdf

Boyd, D., Smith, A. F., & Veale, B. (2000). Flood Management on the Grand River Basin, 1–26.

Brooks, G.R., S.G. Evans and J.J. Clague. (2001). "Flooding". *A Synthesis of Natural Geological Hazards in Canada*. G.R. Brooks (ed.). Ottawa: Geological Survey of Canada Bulletin 548. 101-143

Chen, C., Haerter, J. O., Hagemann, S., & Piani, C. (2011). On the contribution of statistical bias correction to the uncertainty in the projected hydrological cycle. *Geophysical Research Letters*, *38*(20), L20403. doi:10.1029/2011GL049318

Chin, D.A.,2006. Water-Resources Engineering.Prentice Hall, New Jersey

Cunderlik, J., and S.P. Simonovic, (2005) "Hydrologic Extremes in South-western Ontario under future climate projections", *Journal of Hydrologic Sciences*, 50(4):631-654.

Cunderlik, J., and S.P. Simonovic, (2007) "Inverse Flood Risk Modeling Under Changing Climatic Conditions", *Hydrological Processes Journal*, 21(5):563-577.

Cunnane, C., 1989. Statistical distributions for flood frequency analysis, Operational Hydrology Report no. 33, World Meteorological Organization, Geneva

Dankers, R., & Feyen, L. (2009). Flood hazard in Europe in an ensemble of regional climate scenarios. *Journal of Geophysical Research*, *114*(D16), D16108. doi:10.1029/2008JD011523

Das, S., & Simonovic, S. P. (2012). Assessment of Uncertainty in Flood Flows under Climate Change Impacts in the Upper Thames River Basin , Canada. *British Journal of Environment & Climate Change*, *2*(4), 318–338.

Debele, B., Srinivasan, R., & Yves Parlange, J. (2007). Accuracy evaluation of weather data generation and disaggregation methods at finer timescales. *Advances in Water Resources*, *30*(5), 1286–1300. doi:10.1016/j.advwatres.2006.11.009

Decker, M., Brunke, M. a., Wang, Z., Sakaguchi, K., Zeng, X., & Bosilovich, M. G. (2012). Evaluation of the Reanalysis Products from GSFC, NCEP, and ECMWF Using Flux Tower Observations. *Journal of Climate*, *25*(6), 1916–1944. doi:10.1175/JCLI-D-11-00004.1

Déry, S. J. (2005). Decreasing river discharge in northern Canada. *Geophysical Research Letters*, *32*(10), L10401. doi:10.1029/2005GL022845

Dessai, S. (2005). Limited sensitivity analysis of regional climate change probabilities for the 21st century. *Journal of Geophysical Research*, *110*(D19), D19108. doi:10.1029/2005JD005919

Ehret, U., Zehe, E., Wulfmeyer, V., Warrach-Sagi, K., & Liebert, J. (2012). *HESS Opinions* "Should we apply bias correction to global and regional climate model data?" *Hydrology and Earth System Sciences*, *16*(9), 3391–3404. doi:10.5194/hess-16-3391-2012

Environment Canada. 2004. Threats to Water Availability in Canada. National Water Research Institute, Burlington, Ontario. NWRI Scientific Assessment Report Series No. 3 and ACSD Science Assessment Series No. 1. 128 p

Eum, H-I., S.P. Simonovic, (2012) "Assessment on Temporal and Spatial Variability of Extreme Rainfall Events for the Upper Thames River Basin in Canada", (available online: 13 May 2011, DOI: 10.1002/hyp.8145), *Hydrological Processes*, 26(4):485-499.

Farwell, J., Boyd, D., & Ryan, T. (2008). Making Watersheds More Resilient to Climate Change A Response in the Grand River Watershed , Ontario Canada.

Fowler, H. and Kilsby, C.: Using regional climate model data to simulate historical and future river flows in northwest England, Climatic Change, 80, 337–367, doi:10.1007/s10584-006-9117-3,2007

Garraway, M. (2011). Guide for Assessment of Hydrologic Effects of Climate Change in Ontario & Future Climate Change Data Sets, 1–19.

Gosling, S. N., Taylor, R. G., Arnell, N. W., & Todd, M. C. (2011). A comparative analysis of projected impacts of climate change on river runoff from global and catchment-scale hydrological models. *Hydrology and Earth System Sciences*, *15*(1), 279–294. doi:10.5194/hess-15-279-2011

Graham, L. P., J. Andréasson, and B. Carlsson (2007), Assessing climate change impacts on hydrology from an ensemble of regional climate mod- els, model scales and linking methods—A case study on the Lule River basin, Clim. Change, 81(S1), 293–307, doi:10.1007/s10584-006-9215-2

Grand River Conservation Authority, 2005. Establishing Environmental Flow Requirements for Selected Streams in the Grand River Watershed. Prepared by the Ontario Ministry of the Environment

Groisman, P.Y., S. Bomin, R.S. Vose, J.H. Lawrimore, P.H. Whitfield, E. F ørland, I. Hannssen-Baur, M.C. Serreze, V.N. Razuvaev and G.V. Alekseev, 2003: "Contemporary climate changes in high latitudes of the northern hemisphere: daily time resolution". Proceedings of the 14th Symposium on Global Change and Climate Variations

Haerter, J. O., Hagemann, S., Moseley, C., & Piani, C. (2011). Climate model bias correction and the role of timescales. *Hydrology and Earth System Sciences*, *15*(3), 1065–1079. doi:10.5194/hess-15-1065-2011

Hagemann, S., Chen, C., Haerter, J. O., Heinke, J., Gerten, D., & Piani, C. (2011). Impact of a Statistical Bias Correction on the Projected Hydrological Changes Obtained from Three GCMs and Two Hydrology Models. *Journal of Hydrometeorology*, *12*(4), 556–578. doi:10.1175/2011JHM1336.1

Hirabayashi, Y., Mahendran, R., Koirala, S., Konoshima, L., Yamazaki, D., Watanabe, S., … Kanae, S. (2013). Global flood risk under climate change. *Nature Climate Change*, *3*(9), 816–821. doi:10.1038/nclimate1911

Hirabayashi, Y., Kanae, S., & Emori, S. (2009). Global projections of changing risks of floods and droughts in a changing climate, *53*(August 2008).

Hosking, J.R.M., Wallis, J.R., 1997. Regional frequency analysis: an approach based on L-moments. Cambridge University Press, Cambridge.

Huber, M., & Knutti, R. (2011). Anthropogenic and natural warming inferred from changes in Earth's energy balance. *Nature Geoscience*, *5*(1), 31–36. doi:10.1038/ngeo1327

Ines, A. V. M., & Hansen, J. W. (2006). Bias correction of daily GCM rainfall for crop simulation studies. *Agricultural and Forest Meteorology*, *138*(1-4), 44–53. doi:10.1016/j.agrformet.2006.03.009

IPCC, 2012: Managing the Risks of Extreme Events and Disasters to Advance Climate Change Adaptation. A Special Report of Working Groups I and II of the Intergovernmental Panel on Climate Change [Field, C.B., V. Barros, T.F. Stocker, D. Qin, D.J. Dokken, K.L. Ebi, M.D. Mastrandrea, K.J. Mach, G.-K. Plattner, S.K. Allen, M. Tignor, and P.M. Midgley (eds.)]. Cambridge University Press, Cambridge, UK, and New York, NY, USA, 582 pp

IPCC, 2007: Climate Change 2007: The Physical Science Basis. Contribution of Working Group I to the Fourth Assessment Report of the Intergovernmental Panel on Climate Change[Solomon, S., D. Qin, M. Manning, Z. Chen, M. Marquis, K.B. Averyt, M. Tignor and H.L. Miller (eds.)]. Cambridge University Press, Cambridge, United Kingdom and New York, NY, USA, 996 pp

IPCC, 2001:Climate Change 2001: The Scientific Basis. Contribution of Working Group I to the Third Assessment Report of the Intergovernmental Panel on Climate Change [Houghton, J.T., Y. Ding, D.J. Griggs, M. Noguer, P.J. van der Linden, X. Dai, K. Maskell, and C.A. Johnson (eds.)]. Cambridge University Press, Cambridge, United Kingdom and New York, NY, USA, 881pp

IPCC, 2000 - Nebojsa Nakicenovic and Rob Swart (Eds.). IPCC Special Report on Emission Scenarios. Cambridge University Press, UK. pp 570

Jakob Themeßl, M., Gobiet, A., & Leuprecht, A. (2011). Empirical-statistical downscaling and error correction of daily precipitation from regional climate models. *International Journal of Climatology*, *31*(10), 1530–1544. doi:10.1002/joc.2168

Jung, I.-W., Chang, H., & Moradkhani, H. (2011). Quantifying uncertainty in urban flooding analysis considering hydro-climatic projection and urban development effects. *Hydrology and Earth System Sciences*, *15*(2), 617–633. doi:10.5194/hess-15-617-2011

Kalnay, E., M. Kanamitsu, R. Kistler, W. Collins, D. Deaven, L. Gandin, M. Iredell, S. Saha, G. White, J. Woollen, Y. Zhu, M. Chelliah, W. Ebisuzaki, W. Higgins, J. Janowiak, K. C. Mo, C. Ropelewski, J. Wang, A. Leetmaa, R. Reynolds, R. Jenne, and D. Joseph, 1996: The NMC/NCAR 40-Year Reanalysis Project". *Bull. Amer. Meteor. Soc.*, 77, 437-471

Kay, a. L., Davies, H. N., Bell, V. a., & Jones, R. G. (2009). Comparison of uncertainty sources for climate change impacts: flood frequency in England. *Climatic Change*, *92*(1-2), 41–63. doi:10.1007/s10584-008-9471-4

Khakbaz, B., Imam, B., Hsu, K., & Sorooshian, S. (2012). From lumped to distributed via semi-distributed: Calibration strategies for semi-distributed hydrologic models. *Journal of Hydrology*, *418-419*, 61–77. doi:10.1016/j.jhydrol.2009.02.021

Kiktev, D., Sexton, D. M. H., Alexander, L., & Folland, C. . (2003). Comparison of Modeled and Observed Trends in Indices of Daily Climate Extremes. *Journal of Climate*, *16*, 3560–3571.

King, L. M. (2012). APPLICATION OF A K-NEAREST NEIGHBOUR WEATHER GENERATOR FOR SIMULATION OF HISTORICAL AND FUTURE Application of a K-nearest neighbour weather generator for simulation of historical and future climate variables in the Upper Thames River basin.

King, L. M., Mcleod, A. I., & Simonovic, S. P. (2012). Simulation of historical temperatures using a multi-site , multivariate block resampling algorithm with perturbation. doi:10.1002/hyp

King, L., S. Irwin, R. Sarwar, A.I., McLeod and S.P. Simonovic, (2012) "The effects of climate change on extreme precipitation events in the Upper Thames River Basin: A comparison of downscaling approaches", *Canadian Water Resources Journal*, 37(3):253-274.

Kingston, D. G., & Taylor, R. G. (2010). Sources of uncertainty in climate change impacts on river discharge and groundwater in a headwater catchment of the Upper Nile Basin, Uganda. *Hydrology and Earth System Sciences*, *14*(7), 1297–1308. doi:10.5194/hess-14-1297-2010

Knutti, R., Furrer, R., Tebaldi, C., Cermak, J., & Meehl, G. a. (2010). Challenges in Combining Projections from Multiple Climate Models. *Journal of Climate*, *23*(10), 2739–2758. doi:10.1175/2009JCLI3361.1

Kouwen, N., Soulis, E. D., Pietroniro, A., Donald, J., & Harrington, R. A. (1993). Grouped Response Units For Distributed Hydrological Modeling. *Journal of Water Resource Planning and Management*, *119*(3), 289–305.

Labat, D., Godd, Y., Probst, J. L., & Guyot, J. L. (2004). Evidence for global runoff increase related to climate warming. *Advances in water resources*, *27*(6), 631–642.

Lang, M., & Bobe, B. (1999). Towards operational guidelines for over-threshold modeling. *Journal of Hydrology*, *225*, 103–117.

Lapp, S., Sauchyn, D., & Wheaton, E. (2008). Institutional Adaptations to Climate Change Project : Future Climate Change Scenarios for the South Saskatchewan River Basin, (November).

Lemmen, D.S.,Warren, F.J., Lacroix, J., and Bush, E., editors (2008): From Impacts to Adaptation: Canada in a Changing Climate 2007; Government of Canada, Ottawa, ON, 448 p

Mahlstein, I., & Knutti, R. (2009). Regional climate change patterns identified by cluster analysis. *Climate Dynamics*, *35*(4), 587–600. doi:10.1007/s00382-009-0654-0

Maraun, D., & Wetterhall, F. (2010). Precipitation downscaling under climate change: Recent developments to bridge the gap between dynamical models and the end user. *Reviews of …*, (2009), 1–34. doi:10.1029/2009RG000314.1.INTRODUCTION

Maxino, C. C., Mcavaney, B. J., Pitman, A. J., & Perkins, S. E. (2008). Ranking the AR4 climate models over the Murray-Darling Basin using simulated maximum temperature , minimum temperature and precipitation, *1112*(August 2007), 1097–1112. doi:10.1002/joc

Mearns, L. O., W. J. Gutowski, R. Jones, L.-Y. Leung, S. McGinnis, A. M. B. Nunes, and Y. Qian: A regional climate change assessment program for North America. *EOS*, Vol. 90, No. 36, 8 September 2009, pp. 311-312

Meehl, G. a., Covey, C., Taylor, K. E., Delworth, T., Stouffer, R. J., Latif, M., McAvaney, B., et al. (2007). THE WCRP CMIP3 Multimodel Dataset: A New Era in Climate Change Research. *Bulletin of the American Meteorological Society*, *88*(9), 1383–1394. doi:10.1175/BAMS-88-9-1383

Mesinger, F., DiMego, G., Kalnay, E., Mitchell, K., Shafran, P. C., Ebisuzaki, W., Jović, D., et al. (2006). North American Regional Reanalysis. *Bulletin of the American Meteorological Society*, *87*(3), 343–360. doi:10.1175/BAMS-87-3-343

Milly, P. C. D., Betancourt, J., Falkenmark, M., Hirsch, R. M., Zbigniew, W., Lettenmaier, D. P., & Stouffer, R. J. (2008). Stationarity Is Dead : Whither Water Management ?, (February), 573–574.

Mortsch, L. (2011). Climate change scenarios for Mon application in water resources impact and adaptation assessments The challenge for water resources practitioners :

Muerth, M. J., Gauvin St-Denis, B., Ricard, S., Velázquez, J. a., Schmid, J., Minville, M., Caya, D., et al. (2012). On the need for bias correction in regional climate scenarios to assess climate change impacts on river runoff. *Hydrology and Earth System Sciences Discussions*, *9*(9), 10205–10243. doi:10.5194/hessd-9-10205-2012

Pathiraja, S., Westra, S., & Sharma, a. (2012). Why continuous simulation? The role of antecedent moisture in design flood estimation. *Water Resources Research*, *48*(6), W06534. doi:10.1029/2011WR010997

Perkins, S. E., Pitman, a. J., Holbrook, N. J., & McAneney, J. (2007). Evaluation of the AR4 Climate Models' Simulated Daily Maximum Temperature, Minimum Temperature, and

Precipitation over Australia Using Probability Density Functions. *Journal of Climate*, *20*(17), 4356–4376. doi:10.1175/JCLI4253.1

Piani, C. and J. O. Haerter (2012), Two dimensional bias correction of temperature and precipitation copulas in climate models., *Geophys. Res. Lett.*, doi:10.1029/2012GL053839, in press

Piani, C., Haerter, J. O., & Coppola, E. (2009). Statistical bias correction for daily precipitation in regional climate models over Europe. *Theoretical and Applied Climatology*, *99*(1-2), 187–192. doi:10.1007/s00704-009-0134-9

Piani, C., Weedon, G. P., Best, M., Gomes, S. M., Viterbo, P., Hagemann, S., & Haerter, J. O. (2010). Statistical bias correction of global simulated daily precipitation and temperature for the application of hydrological models. *Journal of Hydrology*, *395*(3-4), 199–215. doi:10.1016/j.jhydrol.2010.10.024

Pierce, D. W., Barnett, T. P., Santer, B. D., & Gleckler, P. J. (2009). Selecting global climate models for regional climate change studies. *Proceedings of the National Academy of Sciences of the United States of America*, *106*(21), 8441–6. doi:10.1073/pnas.0900094106

Prodanovic, P. and S.P. Simonovic, (2007)"Impacts of Changing Climatic Conditions in the Upper Thames River Basin" *Canadian Water Resources Journal*, 32(4):265-284.

R Development Core Team (2008). R: A language and environment for statistical computing. R Foundation for Statistical Computing, Vienna, Austria. ISBN 3-900051-07-0, URL http://www.R-project.org.

Raje, D., & Mujumdar, P. P. (2011). A comparison of three methods for downscaling daily precipitation in the Punjab region. *Hydrological Processes*, *25*(23), 3575–3589. doi:10.1002/hyp.8083

Report of the Expert Panel on Climate Change Adaptation (2009). Adapting to Climate Change in Ontario. Retrieved from http://www.ene.gov.on.ca/stdprodconsume/groups/lr/@ene/@resources/documents/resource/std01_079212.pdf

Rojas, R., Feyen, L., Dosio, a., & Bavera, D. (2011). Improving pan-european hydrological simulation of extreme events through statistical bias correction of RCM-driven climate simulations. *Hydrology and Earth System Sciences Discussions*, *8*(2), 3883–3936. doi:10.5194/hessd-8-3883-2011

Schmidli, J., Frei, C., & Vidale, P. L. (2006). Downscaling from GCM precipitation: a benchmark for dynamical and statistical downscaling methods. *International Journal of Climatology*, *26*(5), 679–689. doi:10.1002/joc.1287

Shabbar, A. and B. Bonsal, 2003: As assessment of changes in winter cold and warm spells over Canada. Natural Hazards, 29, 173-188

Sharma, D., Das Gupta, a., & Babel, M. S. (2007). Spatial disaggregation of bias-corrected GCM precipitation for improved hydrologic simulation: Ping River Basin, Thailand. *Hydrology and Earth System Sciences Discussions*, *4*(1), 35–74. doi:10.5194/hessd-4-35-2007

Shrubsole,D. and others (2003). "An assessment of flood risk management in Canada". ICLR Research Paper Series – No. 28. ISBN 0-9732213-6-4

Solaiman, T.A., S. P. Simonovic, and D. H. Burn, (2012) "Quantifying Uncertainties in the Modelled Estimates of Extreme Precipitation Events at Upper Thames River Basin", *British Journal of Environment and Climate Change,* 2(2):180-215.

Solaiman, T., L. King, and S.P. Simonovic, (2010) "Extreme Precipitation Vulnerability in the Upper Thames River Basin: Uncertainty in Climate Model Projections", *International Journal of Climatology,* Published online in Wiley Online Library (wileyonlinelibrary.com) DOI: 10.1002/joc.2244, 31(5), 2011.

Srivastav, R. and S.P. Simonovic, (2013) "Maximum Entropy Bootstrap based Multi-site, Multivariate Weather Generator", submitted to *Journal of Hydrology.*

Stadnyk-Falcone, T. A. (2008). Mesoscale Hydrological Model Validation and Verification using Stable Water Isotopes : The isoWATFLOOD Model.

Swainson, B. (2009). Rivers at Risk :The Status of Environmental Flows in Canada.

Taylor, K. E., Stouffer, R. J., & Meehl, G. a. (2012). An Overview of CMIP5 and the Experiment Design. *Bulletin of the American Meteorological Society*, *93*(4), 485–498. doi:10.1175/BAMS-D-11-00094.1

Taylor, K., "IPCC Coupled Model Output For Working Group 1", IPCC Working Group I Fourth Assessment Report First Lead Authors Meeting. 26-29 September 2004, Trieste, Italy

Tebaldi, C. (2004). Regional probabilities of precipitation change: A Bayesian analysis of multimodel simulations. *Geophysical Research Letters*, *31*(24), L24213. doi:10.1029/2004GL021276

Teutschbein, C., & Seibert, J. (2012). Is bias correction of Regional Climate Model (RCM) simulations possible for non-stationary conditions? *Hydrology and Earth System Sciences Discussions*, *9*(11), 12765–12795. doi:10.5194/hessd-9-12765-2012

Vannitsem, S. (2011). Bias correction and post-processing under climate change. *Nonlinear Processes in Geophysics*, *18*(6), 911–924. doi:10.5194/npg-18-911-2011

Watanabe, S., Kanae, S., Seto, S., Yeh, P. J.-F., Hirabayashi, Y., & Oki, T. (2012). Intercomparison of bias-correction methods for monthly temperature and precipitation simulated by multiple climate models. *Journal of Geophysical Research, 117*(D23), D23114. doi:10.1029/2012JD018192

Whitfield, P. H., & Cannon, A. J. (2000). Recent Variations in Climate and Hydrology in Canada, (1).

Wilby, R. L., & Harris, I. (2006). A framework for assessing uncertainties in climate change impacts: Low-flow scenarios for the River Thames, UK. *Water Resources Research, 42*(2), W02419. doi:10.1029/2005WR004065

Willems, P. (2009). Environmental Modelling & Software A time series tool to support the multi-criteria performance evaluation of rainfall-runoff models. *Environmental Modelling and Software, 24*(3), 311–321. doi:10.1016/j.envsoft.2008.09.005

Young, K. C. (1993).A multivariate chain model for simulating climatic parameters from daily data, Journal of Applied Meteorology, 33, 661-671.

Yukiko hirabayashi, Shinjiro kanae, Seita emori, Taikan Oki & Masahide Kimoto (2008): Global projections of changing risks of floods and droughts in a changing climate, Hydrological Sciences Journal, 53:4, 754-772

APPENDICES

A. Choosing appropriate spatial scale for selection of hydro-climatic extreme scenarios within Ontario province

To highlight the impact of the choice of a suitable spatial scale while selecting extreme scenarios, province of Ontario is divided into three regions with distinct climate types. This is done by using plots of spatial variability in mean annual precipitation and temperature across Ontario as shown in Figure A1.

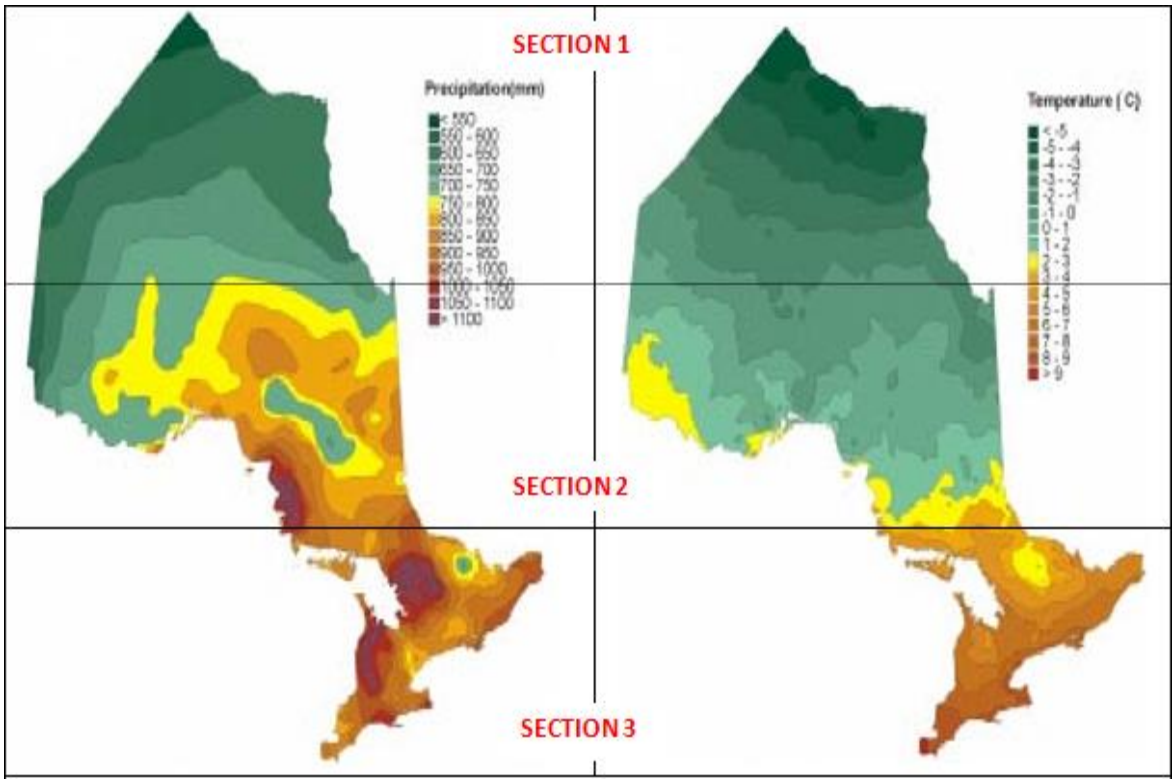

Figure A1. Annual mean daily precipitation and temperature across Ontario (after Baldwin et al., 2000)

B. Gauging stations lying within the Grand River at Brantford

Table B1 List of gauging stations considered in the analysis

Station Name	Long(degrees)	Lat(degrees)	Elevation
Apps mill	-80.383	43.133	230.1
Arthur	-80.567	43.817	452
Ayr	-80.45	43.283	289.6
Blue acton	-80.05	43.6	365.8
Blue corwhin	-80.117	43.533	350.5
Blue rockwood	-80.117	43.583	350.5
Blue scout	-80.083	43.617	342.9
Blue springs creek	-80.117	43.633	373.4
Brantford morell	-80.283	43.15	198.1
Burford	-80.433	43.1	259.1
Cambridge galt moe	-80.317	43.33	268.2
Cambridge-stewart	-80.3	43.35	289
Canning	-80.45	43.183	259.1
Cathcart	-80.567	43.117	269.7
Crewsons corners	-80.1	43.617	358.1
Damascus	-80.483	43.917	487.7
Drumbo	-80.55	43.233	304.8
Drumbo harrington	-80.517	43.233	281.9
Elmira	-80.533	43.6	350.5
Elora automatic climate station	-80.417	43.65	376.4
Elora rcs	-80.417	43.65	376.4
Elora research stn	-80.417	43.65	376.4
Falkland	-80.45	43.133	262.1
Fergus moe	-80.38	43.702	396.2
Fergus shand dam	-80.331	43.735	417.6
Glen allan	-80.711	43.684	400
Grand valley wpcp	-80.333	43.883	464.8
Guelph arboretum	-80.217	43.55	327.7
Guelph oac	-80.233	43.517	333.8
Guelph oac physics dept	-80.267	43.55	340.5
Guelph turfgrass cs	-80.217	43.55	325
Haysville	-80.633	43.35	320
Hillsburgh	-80.167	43.767	427
Kitchener	-80.5	43.433	320
Kitchener city eng 1	-80.483	43.45	320
Kitchener city eng 2	-80.483	43.45	281.9
Kitchener owrc	-80.433	43.4	321.6

Kitchener/waterloo	-80.379	43.461	342.9
Millers lake	-80.383	43.283	304.8
Monticello	-80.4	43.967	481.6
Morriston	-80.117	43.467	304.8
Newton	-80.9	43.583	373.4
Newton	-80.883	43.583	382
Paris	-80.45	43.183	266.7
Preston	-80.417	43.4	291.1
Preston wpcp	-80.35	43.383	272.8
Salem	-80.47	43.71	430
Waldemar	-80.283	43.883	449.6
Waterloo fire hall	-80.517	43.467	317
Waterloo wellington a	-80.383	43.45	317
Waterloo wellington 2	-80.383	43.45	313.6
Waterloo wpcp	-80.517	43.483	327.7

C. Description of climate models considered in the analysis

Table C1 Climate models considered in this study

S.No	Model	Atmospheric component resolution	
		Horizontal(lat x lon)	*Vertical (levels)*
1	BCCR-BCM2.0, 2005	1.9º x 1.9º	L31
2	CGCM3.1(T47), 2005	2.8º x 2.8º	L31
3	CGCM3.1(T63), 2005	1.9º x 1.9º	L31
4	CNRM-CM3, 2004	1.9º x 1.9º	L45
5	CSIRO-MK3.0, 2001	1.9º x 1.9º	L18
6	CSIRO-MK3.5, 2005	1.9º x 1.9º	L18
7	GFDL-CM2.0, 2005	2.0ºx 2.5º	L24
8	GFDL-CM2.1, 2005	2.0º x 2.5º	L24
9	GISS-ER, 2004	4º x 5º	L20
10	IAP-FGOALS, 2004	2.8º x 2.8º	L26
11	INGV-ECHAM4, 2005	1.9º x 1.9º	L18
12	IPSL-CM4, 2005	2.5° x 3.75°	L19
13	MIROC3.2(medres), 2004	2.8º x 2.8º	L20
14	MPI-ECHAM5, 2005	1.9º x 1.9º	L31
15	MRI-CGCM2.3.2, 2003	2.8º x 2.8º	L30

D. Stations at which hourly precipitation data is obtained from the GRCA

Table D1 Stations at which hourly precipitation data is obtained from the GRCA

Station_ID	Station_Name	Easting	Northing
1	Proton Station	538657	4890504
2	Monticello	546796	4870194
3	Grand Valley WPCP	553569	4859138
4	Fergus Shand Dam	553704	4842478
5	Elora RCS	547057	4833173
6	Mount Forest (AUT)	520063	4870059
7	Glen Allan	522851	4836748
8	Elmira	537659	4831262
9	Waterloo Wellington	549910	4810980
10	Preston	547252	4805408
11	Guelph Turfgrass	563292	4822199
12	Cambridge Galt MOE	555396	4797843
13	Stratford MOE	500013	4801541
14	Roseville	543238	4799828
15	Woodstock	520352	4773808
16	Scotland	547562	4760987
17	Brantford MOE	562370	4775914
18	Valens	570216	4803756
19	Middleport	578658	4774231
20	Hagersville	576132	4757543
21	Dunville Pumping stn.	613076	4743243

E. R programming language codes used

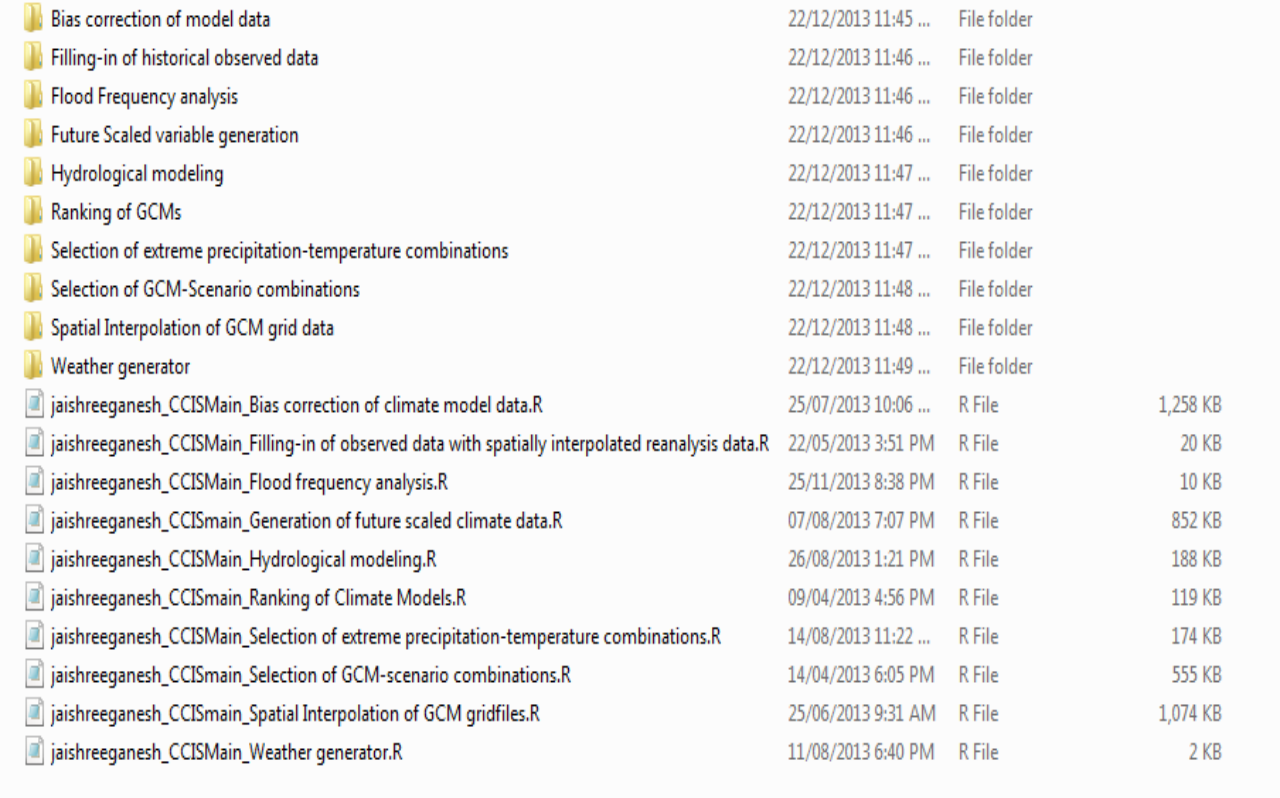

Bias correction of model data	22/12/2013 11:45 ...	File folder	
Filling-in of historical observed data	22/12/2013 11:46 ...	File folder	
Flood Frequency analysis	22/12/2013 11:46 ...	File folder	
Future Scaled variable generation	22/12/2013 11:46 ...	File folder	
Hydrological modeling	22/12/2013 11:47 ...	File folder	
Ranking of GCMs	22/12/2013 11:47 ...	File folder	
Selection of extreme precipitation-temperature combinations	22/12/2013 11:47 ...	File folder	
Selection of GCM-Scenario combinations	22/12/2013 11:48 ...	File folder	
Spatial Interpolation of GCM grid data	22/12/2013 11:48 ...	File folder	
Weather generator	22/12/2013 11:49 ...	File folder	
jaishreeganesh_CCISMain_Bias correction of climate model data.R	25/07/2013 10:06 ...	R File	1,258 KB
jaishreeganesh_CCISMain_Filling-in of observed data with spatially interpolated reanalysis data.R	22/05/2013 3:51 PM	R File	20 KB
jaishreeganesh_CCISMain_Flood frequency analysis.R	25/11/2013 8:38 PM	R File	10 KB
jaishreeganesh_CCISmain_Generation of future scaled climate data.R	07/08/2013 7:07 PM	R File	852 KB
jaishreeganesh_CCISMain_Hydrological modeling.R	26/08/2013 1:21 PM	R File	188 KB
jaishreeganesh_CCISmain_Ranking of Climate Models.R	09/04/2013 4:56 PM	R File	119 KB
jaishreeganesh_CCISMain_Selection of extreme precipitation-temperature combinations.R	14/08/2013 11:22 ...	R File	174 KB
jaishreeganesh_CCISmain_Selection of GCM-scenario combinations.R	14/04/2013 6:05 PM	R File	555 KB
jaishreeganesh_CCISmain_Spatial Interpolation of GCM gridfiles.R	25/06/2013 9:31 AM	R File	1,074 KB
jaishreeganesh_CCISMain_Weather generator.R	11/08/2013 6:40 PM	R File	2 KB

Figure E1. Files layout inside the attached CD-ROM

CD-ROM attached with this blue book contains R-codes used in this research. Codes have been divided into "Main" and "subordinate" categories. "Main" R-codes are associated with a jaishreeganesh_CCISMain_STEPNAME.R structure in their filenames. These files correspond to different steps performed during the climate change analysis. One file each for the steps: Bias correction, Filling-in of observed data using spatially interpolated reanalysis data, flood frequency analysis, generation of future scaled climate data, hydrological modeling, ranking of climate models, selection of extreme precipitation-temperature combinations, selection of GCM-scenario

combinations, spatial interpolation of GCM gridfiles, weather generator is located inside the folder "R-Codes used" in the CD-ROM.

Subordinate R-codes for each step (which are called in the main R-codes) are located in //R-Codes used/STEPNAME folder. The locations of these files and other input files need to be updated in the "Main" R-codes before running them. Codes provided are very generic and can be utilised for performing climate change impact study at any area of interest. Also, separate files are made available for each step so that they can even be utilised when only a section of the analysis is being performed.

F. List of Previous Reports in the Series

ISSN: (print) 1913-3200; (online) 1913-3219
In addition to 58 previous reports (no. 01 – no. 58) prior to 2008;

(1) Evan G. R. Davies and Slobodan P. Simonovic (2008). An integrated system dynamics model for analyzing behaviour of the social-economic-climatic system: Model description and model use guide. Water Resources Research Report no. 059, Facility for Intelligent Decision Support, Department of Civil and Environmental Engineering, London, Ontario, Canada, 233 pages. ISBN: (print) 978-0-7714-2679-7; (online) 978-0-7714-2680-3.

(2) Vasan Arunachalam (2008). Optimization Using Differential Evolution. Water Resources Research Report no. 060, Facility for Intelligent Decision Support, Department of Civil and Environmental Engineering, London, Ontario, Canada, 42 pages. ISBN: (print) 978-0-7714- 2689-6; (online) 978-0-7714-2690-2.

(3) Rajesh Shrestha and Slobodan P. Simonovic (2009). A Fuzzy Set Theory Based Methodology for Analysis of Uncertainties in Stage-Discharge Measurements and Rating Curve. Water Resources Research Report no. 061, 44 Facility for Intelligent Decision Support, Department of Civil and Environmental Engineering, London, Ontario, Canada, 104 pages. ISBN: (print) 978-0-7714-2707-7; (online) 978-0-7714-2708-4.

(4) Hyung-Il Eum, Vasan Arunachalam and Slobodan P. Simonovic (2009). Integrated Reservoir Management System for Adaptation to Climate Change Impacts in the Upper Thames River Basin. Water Resources Research Report no. 062, Facility for Intelligent Decision Support, Department of Civil and Environmental Engineering, London, Ontario, Canada, 81 pages. ISBN: (print) 978-0-7714-2710-7; (online) 978-0-7714-2711-4.

(5) Evan G. R. Davies and Slobodan P. Simonovic (2009). Energy Sector for the Integrated System Dynamics Model for Analyzing Behaviour of the Social- Economic-Climatic Model. Water Resources Research Report no. 063. Facility for Intelligent Decision Support, Department of Civil and Environmental Engineering, London, Ontario, Canada. 191 pages. ISBN: (print) 978-0-7714-2712-1; (online) 978-0-7714-2713-8.

(6) Leanna King, Tarana Solaiman, and Slobodan P. Simonovic (2009). Assessment of Climatic Vulnerability in the Upper Thames River Basin. Water Resources Research Report no. 064, Facility for Intelligent Decision Support, Department of Civil and Environmental Engineering, London, Ontario, Canada, 61pages. ISBN: (print) 978-0-7714-2816-6; (online) 978-0-7714- 2817-3.

(7) Slobodan P. Simonovic and Angela Peck (2009). Updated Rainfall Intensity Duration Frequency Curves for the City of London under Changing Climate. Water Resources Research Report no. 065, Facility for Intelligent Decision Support, Department of Civil and Environmental Engineering, London, Ontario, Canada, 64pages. ISBN: (print) 978-0-7714-2819-7; (online) 987-0-7714-2820-3.

(8) Leanna King, Tarana Solaiman, and Slobodan P. Simonovic (2010). Assessment of Climatic Vulnerability in the Upper Thames River Basin: Part 2. Water Resources Research Report no. 066, Facility for Intelligent Decision Support, Department of Civil and Environmental Engineering, London, Ontario, Canada, 72pages. ISBN: (print) 978-0-7714-2834-0; (online) 978-0-7714-2835-7.

(9) Christopher J. Popovich, Slobodan P. Simonovic and Gordon A. McBean (2010). Use of an Integrated System Dynamics Model for Analyzing Behaviour of the Social-Economic-Climatic System in Policy Development. Water Resources Research Report no. 067, Facility for Intelligent Decision Support, Department of Civil and Environmental Engineering, London, Ontario, Canada, 37 pages. ISBN: (print) 978-0-7714-2838-8; (online) 978-0-7714-2839-5.

(10) Hyung-Il Eum and Slobodan P. Simonovic (2009). City of London: Vulnerability of Infrastructure to Climate Change; Background Report 1 – Climate and Hydrologic Modeling. Water Resources Research Report no. 068, Facility for Intelligent Decision Support, Department of Civil and Environmental Engineering, London, Ontario, Canada, 102pages. ISBN: (print) 978-0-7714-2844-9; (online) 978-0-7714-2845-6.

(11) Dragan Sredojevic and Slobodan P. Simonovic (2009). City of London: Vulnerability of Infrastructure to Climate Change; Background Report 2 – Hydraulic Modeling and Floodplain Mapping. Water Resources Research Report no. 069, Facility for Intelligent Decision Support, Department of Civil and Environmental Engineering, London, Ontario, Canada, 147 pages. ISBN: (print) 978-0-7714-2846-3; (online) 978-0-7714-2847-0.

(12) Tarana A. Solaiman and Slobodan P. Simonovic (2011). Quantifying Uncertainties in the Modelled Estimates of Extreme Precipitation Events at the Upper Thames River Basin. Water Resources Research Report no. 070, Facility for Intelligent Decision Support, Department of Civil and Environmental Engineering, London, Ontario, Canada, 167 pages. ISBN: (print) 978-0-7714-2878-4; (online) 978-0-7714-2880-7.

(13) Tarana A. Solaiman and Slobodan P. Simonovic (2011). Assessment of Global and Regional Reanalyses Data for Hydro-Climatic Impact Studies in the Upper Thames River Basin. Water Resources Research Report no. 071, Facility for Intelligent Decision Support, Department of Civil and Environmental Engineering, London, Ontario, Canada, 74 pages. ISBN: (print) 978-0-7714-2892-0; (online) 978-0-7714-2899-9.

(14) Tarana A. Solaiman and Slobodan P. Simonovic (2011). Development of Probability Based Intensity-Duration-Frequency Curves under Climate Change. Water Resources Research Report no. 072, Facility for Intelligent Decision Support, Department of Civil and Environmental Engineering, London, Ontario, Canada, 89 pages. ISBN: (print) 978-0-7714-2893-7; (online) 978-0-7714-2900-2.

(15) Dejan Vucetic and Slobodan P. Simonovic (2011). Water Resources Decision Making Under Uncertainty. Water Resources Research Report no. 073, Facility for Intelligent Decision Support, Department of Civil and Environmental Engineering, London, Ontario, Canada, 143 pages. ISBN: (print) 978-0-7714-2894-4; (online) 978-0-7714-2901-9.

(16) Angela Peck, Elisabeth Bowering and Slobodan P. Simonovic (2010). City of London: Vulnerability of Infrastructure to Climate Change, Final Report - Risk Assessment. Water Resources Research Report no. 074, Facility for Intelligent Decision Support, Department of Civil and Environmental Engineering, London, Ontario, Canada, 66 pages. ISBN: (print) 978-0-7714-2895-1; (online) 978-0-7714-2902-6.

(17) Akhtar, M. K., S. P. Simonovic, J. Wibe, J. MacGee, and J. Davies, (2011). An integrated system dynamics model for analyzing behaviour of the social-energy-economic-climatic system: model description. Water Resources Research Report no. 075, Facility for Intelligent Decision Support, Department of Civil and Environmental Engineering, London, Ontario, Canada, 211 pages. ISBN: (print) 978-0-7714-2896-8; (online) 978-0-7714-2903-3.

(18) Akhtar, M. K., S. P. Simonovic, J. Wibe, J. MacGee, and J. Davies, (2011). An integrated system dynamics model for analyzing behaviour of the social-energy-economic-climatic system: user's manual. Water Resources Research Report no. 076, Facility for Intelligent Decision Support, Department of Civil and Environmental Engineering, London, Ontario, Canada, 161 pages. ISBN: (print) 978-0-7714-2897-5; (online) 978-0-7714-2904-0.

(19) Millington, N., S. Das and S. P. Simonovic (2011). The Comparison of GEV, Log-Pearson Type 3 and Gumbel Distributions in the Upper Thames River Watershed under Global Climate Models. Water Resources Research Report no. 077, Facility for Intelligent Decision Support, Department of Civil and Environmental Engineering, London, Ontario, Canada, 53 pages. ISBN: (print) 978-0-7714-2898-2; (online) 978-0-7714-2905-7.

(20) Andre Schardong and Slobodan P. Simonovic (2012). Multi-objective Evolutionary Algorithms for Water Resources Management. Water Resources Research Report no. 078, Facility for Intelligent Decision Support, Department of Civil and Environmental Engineering, London, Ontario, Canada, 167 pages. ISBN: (print) 978-0-7714-2907-1; (online) 978-0-7714-2908-8.

(21) Samiran Das and Slobodan P. Simonovic (2012). Assessment of Uncertainty in Flood Flows under Climate Change: the Upper Thames River basin (Ontario, Canada). Water Resources Research Report no. 079, Facility for Intelligent Decision Support, Department of Civil and Environmental Engineering, London, Ontario, Canada, 67 pages. ISBN: (print) 978-0-7714-2960-6; (online) 978-0-7714-2961-3.

(22) Rubaiya Sarwar, Sarah E. Irwin, Leanna M. King and Slobodan P. Simonovic (2012). Assessment of Climatic Vulnerability in the Upper Thames River basin: Downscaling with SDSM. Water Resources Research Report no. 080, Facility for Intelligent Decision Support, Department of Civil and Environmental Engineering, London, Ontario, Canada, 65 pages. ISBN: (print) 978-0-7714-2962-0; (online) 978-0-7714-2963-7.

(23) Sarah E. Irwin, Rubaiya Sarwar, Leanna King and Slobodan P. Simonovic (2012).Assessment of Climatic Vulnerability in the Upper Thames River basin: Downscaling with LARS-WG. Water Resources Research Report no. 081, Facility for Intelligent Decision Support, Department of Civil and Environmental Engineering, London, Ontario, Canada, 80 pages. ISBN: (print) 978-0-7714-2964-4; (online) 978-0-7714-2965-1.

(24) Samiran Das and Slobodan P. Simonovic. (2012). Guidelines for Flood Frequency Estimation under Climate Change. Water Resources Research Report no. 082, Facility for Intelligent Decision Support, Department of Civil and Environmental Engineering, London, Ontario, Canada, 44 pages. ISBN: (print) 978-0-7714-2973-6; (online) 978-0-7714-2974-3.

(25) Angela Peck and Slobodan P. Simonovic. (2013). Coastal Cities at Risk (CCaR): Generic System Dynamics Simulation Models for Use with City Resilience Simulator. Water Resources Research Report no. 083, Facility for Intelligent Decision Support, Department of Civil and Environmental Engineering, London, Ontario, Canada, 55 pages. ISBN: (print) 978-0-7714-3024-4; (online) 978-0-7714-3025-1.